ELSEVIER

Lithos 60 (2002) 89–111

LITHOS

www.elsevier.com/locate/lithos

Crystal-melt equilibria involving potassium-bearing clinopyroxene as indicator of mantle-derived ultrahigh-potassic liquids: an analytical review

L.L. Perchuk [a,b,*], O.G. Safonov [a,b], V.O. Yapaskurt [a], J.M. Barton Jr. [c]

[a] *Department of Petrology, Moscow State University, Moscow 119899 Russia*
[b] *Institute of Experimental Mineralogy of Russian Academy of Sciences, Chernogolovka, Moscow 142432, Russia*
[c] *Department of Geology, Rand Afrikaans University, P.O. Box 524, Auckland Park 2006, South Africa*

Received 17 September 2000; accepted 15 June 2001

Abstract

Crystal–liquid equilibria, including phase relationships of minerals with silicate and/or carbonate melts, are reviewed in order to understand the occurrence of clinopyroxene with up to 2 wt.% K_2O (*KCpx*). This mineral occurs as inclusions in diamond from kimberlite pipes and in garnet from garnet–clinopyroxene potassium-poor silicate rocks intercalated with diamondiferous silicate–carbonate rocks of the Kokchetav Complex, northern Kazakhstan. The analysis of the available experimental data allowed estimation of the effect of *P*, *T* and compositional parameters on the equilibrium of $KAlSi_2O_6$ (in *Cpx*) = $1/4K_4Si_2O_6 + 3/4Al_{4/3}Si_2O_6$ (in *melt*) in various silicate systems. A strong dependence of the K_2O partition coefficient both on pressure and SiO_2 and Al_2O_3 contents in the melt was identified and thermodynamically described. The resulting thermodynamic equation allows the calculation of pressure of the *KCpx* formation within interval 50–100 kbar for known melt compositions. A model for the formation of *KCpx* in deep-mantle potassium-rich carbonate–silicate magmas was derived using the available experimental and petrologic data. The formation of *KCpx* from any potassium-poor ($K_2O < 0.2$ wt.%) melt is impossible because the partition coefficient, $K_p^{Cpx/L} = K_2O$ in *Cpx*/K_2O of melt is much smaller then 1. The presence of *Cpx* with 1 wt.% of K_2O as inclusions in *Grt* from potassium-poor rocks could be explained only by the crystallization of *KCpx* from potassium-rich silicate or silicate–carbonate magma in the presence of KCl brine at $P > 70$ kbar. This chemical zoning of potassium-bearing clinopyroxene suggests its crystallization together with feldspar from silicate melt during rapid ascent of melt toward the Earth's surface from depth about 200 km. Since Tschermak-type substitution has not been observed in either pyroxene, we suggested that feldspar resulted from the peritectic reaction $KAlSi_2O_6 + [SiO_2]_{L/fl} = KAlSi_3O_8$ at relatively shallow mantle levels. A hypothetical phase diagram for the system $Ca(Mg,Fe)Si_2O_6$–$KAlSi_2O_6$ is presented.

Keywords: Mineral equilibria; Potassium-bearing clinopyroxene; Inclusions; Mantle; Melting relations

1. Introduction

A possible way to understand the sources of potassium in the Earth's mantle is to consider the origin of potassium-rich rocks, such as fergusites, leucite basalts, leucitites, etc., as well as kimberlites and lam-

* Corresponding author. Department of Petrology, Geological Faculty, Moscow State University, Vorobievy Gory, Moscow 119899, Russia. Tel.: +7-09-593-91305; fax: +7-09-593-28889.
E-mail addresses: llp@geol.msu.ru (L.L. Perchuk), oleg@iem.ac.ru (O.G. Safonov), jmb@na.rau.ac.za (J.M. Barton Jr.).

0024-4937/02/$ - see front matter
PII: S0024-4937(01)00072-X

proites. Kushiro (1980) showed that an increase of pressure causes an appreciable displacement of the cotectic toward kalsilite in the system Mg_2SiO_4-$KAlSiO_4$-SiO_2. That should assist the formation of potassium-rich magmas at mantle pressure. Addition of water into the system results in a decrease of the liquidus temperature, but does not change the effect of pressure on expansion of the primary crystallization fields of olivine and orthopyroxene at the expense of kalsilite (Perchuk, 1987). Thus, pressure (P) is the most important parameter that regulates the formation of highly potassic magmas. Such magmas are characteristic for rifts (e.g., eastern Africa, the Rhein trough, and northern Baikal) and occur locally in some fold belts (e.g., the Pamirs) and subduction zones (northern Indonesia and Italy). However, ultra-high pressure minerals such as diamond, coesite, potassium-bearing clinopyroxene, etc., are not found as phenocrysts in these rocks. That implies that the generation of the initial magmas occurred in depths less than 100 km. According to the data on melt inclusions (Kogarko et al., 1991; Solovova et al., 1996; Nielsen et al., 1997), such magmas originate in the upper mantle, but beyond the diamond stability field (Wyllie and Lee, 1998).

Microinclusions of potassium-bearing clinopyroxene (*KCpx*) and fluids are common in diamonds from kimberlite pipes (e.g., Reid et al., 1976; Bishop et al., 1978; Navon et al., 1988; Harlow and Veblen, 1991; Israeli et al., in press). The presence of such inclusions created no theoretical problems until the data on inclusions of *KCpx* from the extremely potassium-poor silicate and calc-silicate rocks of the Kokchetav Complex, northern Kazakhstan, appeared (Sobolev and Shatsky, 1990; Perchuk et al., 1995, 1996). These problems are as follows. Firstly, according to experimental data, *KCpx* is stable at $P \gg 40$ kbar and 1200–1500 °C (Table 1). Therefore, its occurrence in crustal metamorphic environments is hard to explain. Secondly, the K_2O partitioning coefficient between *KCpx* and a melt of any composition is always less then 1.0. Thus, *Cpx* cannot be richer in K_2O than the rocks in which it occurs, unless it is residue of some primary K-rich melt, subsequently removed from the rocks. Thus, the occurrence of *KCpx* implies unusual circumstances. Perchuk and Yapaskurt (1998) proposed that at mantle

Table 1
Run conditions for the synthesis of potassium-bearing clinopyroxenes in the model and natural systems

Reference	T (°C)	P (kbar)	System	Na_2O (wt.%)	K_2O (wt.%)	
				System before run	System before run	*Cpx*[a]
Alumino-silicate systems						
Erlank and Kushiro (1970)	1000–1450	15–30.5	*Di–Phl, Kfs–An*$_{50}$*Fo*$_{50}$	0	?	0.05–0.14
Shimizu (1971)	1400, 1350	38–100	*Di*$_{50}$*Fo*$_{13.5}$ + *An*$_{25.5}$*Phl*$_{10}$	0	1.2	0.42–2.2
Shimizu (1974)	1100–1200	15–30	a model system *Di* + *An* + K_2O	0	2.2	< 0.01
Luth (1992)	1200–1500	50–110	model systems *Di* + $KAlSi_2O_6$ and *Di* + $KCrSi_2O_6 \pm H_2O$	?	?	0.13–2.0
Edgar and Vukadinovic (1993)	1250–1500	50–60	armalcolite–phlogopite lamproite	0.96	8.84	0.12–1.67
Mitchell (1995)	1000–1700	40–70	sanidine-phlogopite lamproite	1.25	11.59	0.34–1.86
Luth (1995, 1997)	1250–1600	30–170	a model system *Phl–Di*	0	5.6	0.13–1.2
Edgar and Mitchell (1997)	900–1200	70–120	armalcolite–phlogopite lamproite	0.96	8.84	0.3–2.59
Okamoto and Maruyama (1998)	900–1200	26–70	eclogite + *Ms*[b]	?	?	0.0–0.23
Tsuruta and Takahashi (1998)	1100–2050	10–125	high-K basalt	2.85	1.46	0.01–1.03
Wang and Takahashi (1999)	1400–2350	25–250	high-K basalt	2.64	1.31	0.0–1.9
Carbonate–silicate systems						
Harlow (1997)	1300–1700	50–140	a model system *Cpx* + K_2CO_3 ($KHCO_3$)	?	?	1.09–4.51
Matveev et al. (1998)	1000–1600	70	a model system $K_2Mg(CO_3)_2$ + *Di* + *Grs*;	0	?	0.56–4.83

?—data unknown.
[a] After run.
[b] *Ms*/rock ratio in the starting material was not given.

conditions *KCpx* could crystallize at liquidus of a potassium-rich carbonate–silicate liquid. The miscibility of the carbonate and silicate liquids decreases as pressure drops (e.g., Lee and Wyllie, 1997), while crystallizing *KCpx* could be captured by any latter mineral, for example garnet.

In this paper, all available experimental and natural data are reviewed in order to:

1. find general dependencies of potassium substitution in *Cpx* on the external parameters and the melt composition;
2. deduce an equation for the dependence of the potassium partition coefficient between silicate melt and *Cpx*, and to calculate *P* and *T* for *KCpx* formation in mantle conditions;
3. preliminarily calculate the high-temperature phase relations of in system $CaMgSi_2O_6$–$KAlSi_2O_6$;
4. evaluate the possibility of *KCpx* crystallization from potassium-rich mantle liquids using the compositions of melt, fluid, and brine inclusions in diamonds from kimberlitic pipes;
5. explore the possibility of the peritectic reaction, producing the clinopyroxene-K-feldspar aggregates in *Cpx* grains from quartz-free rocks of the Kokchetav Complex (Perchuk et al., 1996) and some diamondiferous eclogites from South Africa (Reid et al., 1976).

2. A review of the existing experimental data on the equilibria involving *KCpx*

Because of the structure of *Cpx*, the coupled substitution of large potassium cation into the M2 site, $(Mg, Fe)^{M1}Ca^{M2} \Leftrightarrow Al^{M1}K^{M2}$, is impossible at low pressure (Harlow, 1996). Therefore, all experimental studies on the *KCpx* synthesis were performed at very high pressures (see Table 1). The experimental studies cover a wide spectrum of system compositions, from alumino-silicate (Erlank and Kushiro, 1970; Shimizu, 1971, 1974; Edgar and Vukadinovic, 1993; Mitchell, 1995; Edgar and Mitchell, 1997; Luth, 1992, 1995, 1997; Okamoto and Maruyama, 1998; Tsuruta and Takahashi, 1998; Wang and Takahashi, 1999) to carbonate–silicate systems (Harlow, 1997; Matveev et al., 1998).

2.1. Alumino-silicate systems

Experiments on the crystallization of *KCpx* in alumino-silicate systems have been conducted in both model and natural systems. Erlank and Kushiro (1970) attempted to synthesize *KCpx* from the mixtures of *APhl* or *Kfs* with diopside or $An_{50}Fo_{50}$ at 1000–1450 °C and 15–30.5 kbar. The maximal K_2O content in diopside coexisting with *Fo* and glass did not exceed 0.14 wt.% at 21 kbar and 1250 °C. At 70 kbar, *KCpx* was absent in the run products.

Shimizu (1971) studied the pressure dependence of the K_2O content in *Cpx* in the sub-solidus system $Di_{50}Fo_{13.5}An_{26.5}APhl_{10}$ at 38 kbar (1350 °C), 72 kbar (1350 °C) and 100 kbar (1400 °C). The maximal K_2O in *Cpx* was 2.2 wt.% at 100 kbar and 1400 °C. Later, Shimizu (1974) studied the partitioning of potassium and some minor elements (Sr, Ba, Rb, Cs) between *Cpx* and melt in the system *Di–An–Ab* at 15–30 kbar and 1100–1200 °C. The concentrations of K, Sr, Ba, Rb, Cs in the system were similar to those of high-K basalts (for example, 2.2 wt.% K_2O). Despite the low K_2O concentrations (maximum is 0.012 K_2O wt.% at 25 kbar and 1100 °C), the partition coefficient of K_2O, K_p, between *KCpx* and L_{Si} steadily increased from 0.0014 at 15 kbar to 0.0026 at 30 kbar. Shimizu's (1971, 1974) experiments clearly demonstrated that K_2O becomes more compatible in *Cpx* with increasing pressure.

In order to determine a maximal solubility of potassium in clinopyroxene, Luth (1992) carried out experiments in quasi-binary joins $CaMgSi_2O_6$–$KAlSi_2O_6$ and $CaMgSi_2O_6$–$KCrSi_2O_6$ at 50–110 kbar and 1200–1500 °C. Following Shimizu's (1971, 1974) conclusions, Luth (1992) found that in the first system concentration of K_2O in *Cpx* increased from 0.13 wt.% at 50 kbar to 0.61 wt.% at 110 kbar at 1300 °C. In the later paper, Luth (1995) reported even 3 wt.% of K_2O in clinopyroxene in the system $CaMgSi_2O_6$–$KAlSi_2O_6$. However, author did not mention conditions of the synthesis of such highly potassic clinopyroxene. In addition, Luth (1992) experimentally confirmed the effectiveness of Cr in stabilization of K in the clinopyroxene structure that was previously described by Harlow and Veblen (1991).

In order to study the relative stability of *Phl* and *Cpx*, Luth (1995, 1997) studied the system *Phl–Di* at 30–170 kbar and 1250–1600 °C. According to his

data, the assemblage *Cpx–Grt–Ol–*L_{Si} is stable from the liquidus to the solidus of the system within the *P* range 60–150 kbar. At lower *P*, this assemblage is replaced by *Cpx–Ol–*L_{Si}. The maximal K_2O content in *Cpx* (1.3 wt.%) was obtained at 170 kbar and 1600 °C, but at $P \leq 50$ kbar the K_2O content in *Cpx* did not exceed 0.3 wt.%. The $K_p^{Cpx/L}$ increases systematically with *P*, whereas a *T* dependence of the $K_p^{Cpx/L}$ was not observed.

Most experimental studies on the *KCpx* synthesis in natural systems were conducted using potassium-rich mantle rocks such as lamproites. Edgar and Vukadinovic (1993) investigated the conditions of the *KCpx* crystallization in a melt of armalcolite–phlogopite lamproite from Smoky Butte. The experiments were carried out at 50 and 60 kbar in the *T* interval 1250–1500 °C. All run products contained glass. Taking into account earlier experiments of Edgar et al. (1992), Edgar and Vukadinovic (1993) constructed a phase diagram including melting relations in the intervals 10–60 kbar and 900–1500 °C. They found that *Cpx* with the highest K_2O content (1.58–1.67 wt.%) formed at 1250–1200 °C and 60 and 50 kbar in the assemblage *Grt + Phl + Ru + Cos +* L_{Si}. With increasing temperature, *Phl* disappears first from the assemblage, being followed by *Cos*. *Cpx* was the only liquidus phase at 50 kbar and 1400 °C. At 60 kbar and 1500 °C, *Grt* and *Cpx* were both stable on the liquidus. *Grt* disappeared below 50–45 kbar, being replaced by *Cpx + Opx* and *Cpx + Phl*. Edgar and Vukadinovic (1993) showed that at high K_2O content in the system and $P > 50$ kbar, relatively low T (< 1300 °C) was most favorable for the crystallization of *KCpx*. However, Harlow (1997) called attention to the dependence of the K_2O concentration in *Cpx* from experiments of Edgar and Vukadinovic (1993) on its enstatite–ferrosilite content, which is negatively correlated with temperature. According to Harlow (1997), an increase of the enstatite–ferrosilite content in *KCpx* causes a decrease in the molar volume of *Cpx*, and this is the only reason for the *T* dependence of the K_2O content in *Cpx* in the experiments of Edgar and Vukadinovic (1993). Later, Edgar and Mitchell (1997) studied the same system at 70–120 kbar and observed no dependence of K_2O content in *Cpx* on temperature. Edgar and Mitchell (1997) found that *KCpx* was stable with garnet at the liquidus within the whole *P* interval. *Opx* and *Ol* appeared only at $P < 50$ kbar. The K_2O content of *KCpx* varied from 0.3 wt.% at 1500 °C and 80 kbar to 2.58 wt.% at 1500 °C and 120 kbar. Edgar and Mitchell (1997) found that the K_2O content of clinopyroxene decreased in presence of K-bearing phases (phlogopite, K–Ti silicates, K–Ba phosphates) near the solidus (1100–1300 °C).

Mitchell (1995) used sanidine-phlogopite lamproite from Leucite Hills for his experiments at 40–70 kbar and 1000–1700 °C, and found that both *Grt* and *Cpx* were present at the liquidus at 1600 °C and above 45 kbar. Coesite, K–Ti silicate, and K–Ba phosphate joined the assemblage below 1400–1500 °C, while *Phl* and K-richterite were stable at 1100 °C. *KCpx* was the only liquidus phase at $P < 45$ kbar. The K_2O content in *Cpx* increased with *P* reaching 1.86 wt.% at 70 kbar and 1400 °C. A dependence of the K_2O content in *Cpx* on temperature was not observed. Sanidine was found at the solidus at $P < 55$ kbar and $T < 1250$ °C. Its formation was accompanied by a significant decrease in the K_2O content in *Cpx*. For example, at 1200 °C, the K_2O content in *Cpx* decreased from 1.03 wt.% at 60 kbar to 0.55 wt.% at 50 kbar.

Tsuruta and Takahashi (1998) and Wang and Takahashi (1999) studied the melting relations of anhydrous alkalic basalt (JB1, $K_2O = 1.31$ wt.% and $Na_2O = 2.64$ wt.%) at pressure up to 200 kbar and 1100–2400 °C. They showed that *KCpx* is the liquidus phase at 10–70 kbar. At $P > 70$ kbar, *Cpx* has been replaced by *Grt*. The following crystallization sequence was observed with decreasing pressure from 10 to 70 kbar: (1) *Cpx*; (2) *Grt* ($P < 40$ kbar) or coesite ($P > 40$ kbar); (3) *San* at temperature 1200–1400 °C and $P < 60$ kbar; (4) the assemblage *Cpx + Grt + San + Cos + Rt* at 1000–1200 °C. An inflection in the solidus within 60–75 kbar was documented. The slope of the solidus line changes from 5°/kbar to 40°/kbar, and subsequently flattens at *P* above 100 kbar to almost 2°/kbar. This behavior resulted from the appearance of *San* which is not stable at $P > 60$ kbar. The K_2O content in *Cpx* increased over 1 wt.% in the *P* interval studied. The K_2O content in *Cpx* was observed to distinctly decrease in presence of melt. *KCpx* with up to 1.03 wt.% K_2O was found to be stable when it was the only potassium-bearing phase. A temperature dependence of the K_2O content in *Cpx* was not observed as well (Tsuruta and Takahashi, 1998).

Okamoto and Maruyama (1998) analyzed *KCpx* at the eclogite solidus obtained for two different samples from the Dabie Shan Complex (Eastern China). Muscovite was added to one sample, and its K_2O content was 9.32 wt.%. The K_2O content of *KCpx* increased at 900 °C from 0.07 wt.% at 30 kbar to 0.23 wt.% at 70 kbar. A similar pattern was observed at 1000 °C. A minor increase of the K_2O content in *Cpx* with temperature was reported.

Konzett and Ulmer (1999) experimentally explored the stability of hydrous potassic phases (phlogopite and K-richterite) at 40–95 kbar and 800–1400 °C in both the analogue system KNCMASH and in natural lherzolite with addition of 5 wt.% of phlogopite or 10 wt.% of K-richterite. Konzett and Ulmer (1999) found that *Cpx* was stable within the all *P–T* interval studied, but the K_2O content in *Cpx* depended critically on the phase assemblage. The K_2O content abruptly decreased to ~ 0.2 wt.% in the presence of phlogopite and to 0.45 wt.% in the presence of K-richterite and/or melt. The K_2O content in *Cpx* from pure lherzolite without any additions of K_2O did not exceed 0.05–0.1 wt.%. The composition of *KCpx* at given *P* and *T* depended only on the bulk K_2O content.

2.2. Carbonate–silicate systems

Only two experimental studies are known on the *KCpx* crystallization in carbonate–silicate systems. Harlow (1997) investigated the partitioning of K_2O between *Cpx* and coexisting carbonate melt in the system $CaMgSi_2O_6$-$NaAlSi_2O_6$-$NaCrSi_2O_6$-K_2CO_3-$KHCO_3$ at 50–110 kbar and 1300–1700 °C, with addition of small amount of quartz and enstatite to it. The choice of such a complex system was based on the results of a study of chromium-bearing *KCpx* inclusions in diamond from some kimberlite pipes of South Africa and Botswana (Harlow and Veblen, 1991). The maximal K_2O contents in *Cpx*, 4.39 and 4.51 wt.%, were observed at pressure 100 kbar for the system $Di_{50}Ko_{50}$–K_2CO_3. As mentioned above, the presence of chromium assisted to the potassium substitution in *Cpx*. Under the same *P–T* conditions, Cr-free *KCpx* was two to three times poorer in K_2O. An X-ray examination study in *Cpx* in the run product showed a dependence of its molar volume on the K_2O content. A similar dependence has been previously found for natural *Cpx* (Harlow and Veblen, 1991). This dependence explains the high K_2O content in the Cr-bearing *Cpx* in comparison to the Cr-free *Cpx*, as well as the influence of sodium on the potassium solubility in *Cpx*. This study also confirmed the dependence of K_p on *P*, while the *T* dependence was not observed. The most important result of Harlow's study is the confirmation of the low K_p in the system *KCpx*–L_c, which varies from 0.03 to 0.071. In other words, *Cpx* with $K_2O > 1$ wt.% can crystallize in equilibrium with the carbonate liquid containing 14–33 wt.% K_2O at any given *T* and *P* within 1300–1700 °C and 50–110 kbar intervals.

Matveev et al. (1998) investigated the stability of *KCpx* at 70 kbar and 1500 and 1600 °C on the liquidus of the carbonate–silicate system $K_2Mg(CO_3)_2$-K_2CO_3-*Di-Grs*, i.e., a synthetic analogue system of the garnet–clinopyroxene–carbonate diamondiferous rocks of the Kokchetav Complex. Beside *KCpx*, the run products contained pyrope-grossular *Grt*, dolomite, and homogeneous silicate glass. The maximal K_2O content in *Cpx* was 4.83 wt.%, i.e., the highest K_2O concentration documented so far.

3. Discussion of the observed potassium solubility in *Cpx*

Although the experiments reviewed above cover a wide range of *P* and *T*, most of the starting compo-

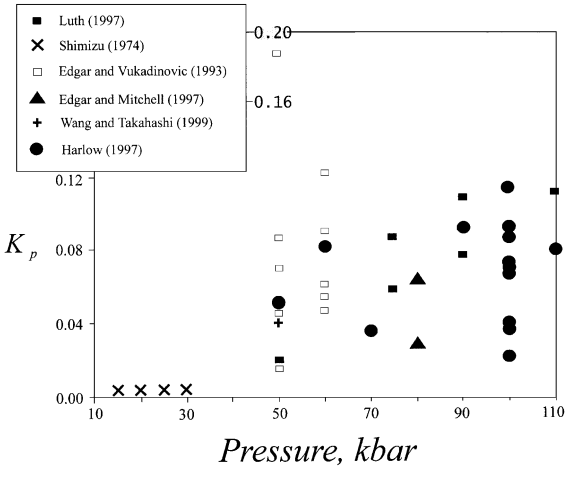

Fig. 1. The variation of the K_2O partition coefficient (K_p) between clinopyroxene and melt according to available experimental data.

sitions did not include simple binary systems, which would allow to constrain specific $P–X$ or $T–X$ phase diagrams involving *KCpx*. The data by Luth (1992) on the join $CaMgSi_2O_6–KAlSi_2O_6$ are very confined. This limits the applicability of the data for a rigorous analysis of the potassium solubility in *Cpx*. Never-

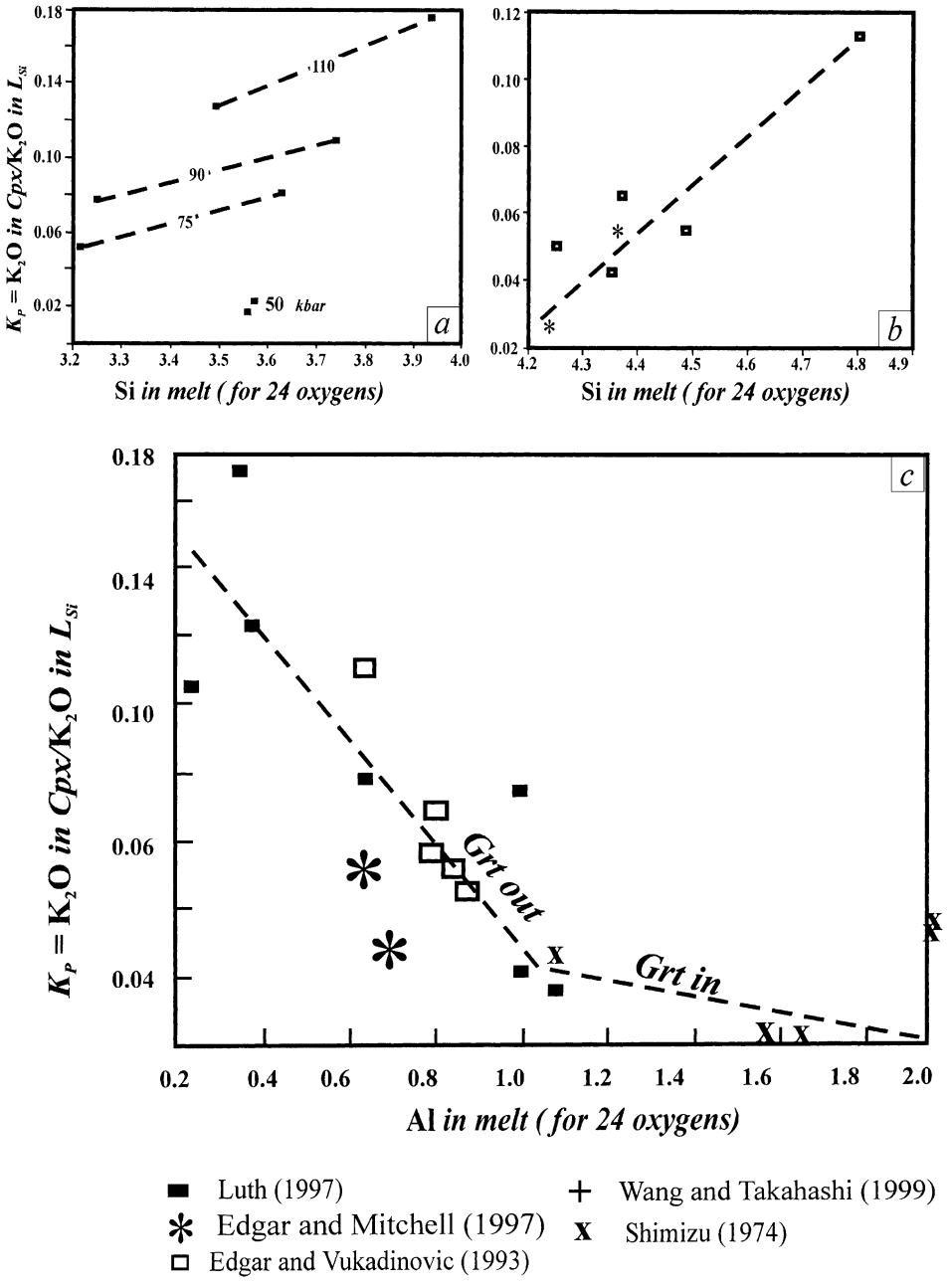

Fig. 2. The variation of the K_2O partition coefficient (K_p) between clinopyroxene and melt with SiO_2 and Al_2O_3 in the silicate melt according to available experimental data (see text for more details).

theless, a semi-quantitative evaluation of the different parameters controlling the *KCpx*-melt equilibrium is possible.

(1) The K partitioning between *Cpx* and melt is *P* dependent in any bulk composition. However, it is impossible to calculate the dependence of $K_p^{Cpx/L}$ on *P* even approximately because of the appreciable scatter in the available data (Fig. 1). Nevertheless, this scatter likely results from the very strong influence of the melt and clinopyroxene compositions on $K_p^{Cpx/L}$.

(2) $K_p^{Cpx/L} \ll 1.0$ for any composition within a wide range of *P* and *T*.

(3) The nature of the *T* dependence of K_2O content in *Cpx* is ambiguous (Mitchell, 1995; Luth, 1997; Edgar and Mitchell, 1997; Tsuruta and Takahashi, 1998).

(4) Existing experimental data indicate that the clinopyroxene from carbonate–silicate melts is richer in K_2O when compared with the clinopyroxene from alumino-silicate melts. Even at $P \approx 200$ kbar, the K_2O concentration in *Cpx* crystallizing from alumino-silicate melts never exceeds 3 wt.% while the K_2O content in *Cpx* above 4 wt.% is observed in carbonate–silicate melts (Harlow, 1997; Matveev et al., 1998). Nevertheless, new experimental studies may change this conclusion.

(5) *KCpx* either does not crystallize or its K_2O content is extremely low in the K_2O-poor alumino-silicate systems ($K_2O < 1$ wt.%; Okamoto and Maruyama, 1998; Konzett and Ulmer, 1999). In contrast, *KCpx* with about 0.5 wt.% may crystallize even at significantly lower *P* in the relatively K_2O-rich systems, such as lamproites (Edgar and Vukadinovic, 1993; Mitchell, 1995; Edgar and Mitchell, 1997).

(6) The K_2O contents in *Cpx* depend both on the bulk composition and the mineral assemblage of a system, e.g., K_2O in *Cpx* abruptly decreases in the presence of K-bearing phases (e.g., Luth, 1995, 1997; Tsuruta and Takahashi, 1998).

(7) $K_p^{Cpx/L}$ depends directly on the SiO_2 (Fig. 2a and b) and inversely on the Al_2O_3 contents (Fig. 2c) of the alumino-silicate melt.

(8) The reciprocal substitution $(Mg,Fe)_{M1}Ca_{M2} \Leftrightarrow (Al,Cr,Fe^{3+})_{M1}K_{M2}$ is the most efficient scheme for potassium incorporation into *Cpx* (Luth, 1992; Edgar and Vukadinovic, 1993; Harlow, 1997).

(9) The potassium solubility in *Cpx* is controlled by its composition, which in turn optimizes the molar volume (Harlow, 1997). Cr-bearing diopside is the most favored, while omphacite is least favored for potassium (Harlow and Veblen, 1991; Luth, 1992; Harlow, 1997).

4. Thermodynamic treatment of the available experimental data for the *KCpx* equilibria in alumino-silicate systems

The available experimental data show that the K_2O content in *Cpx* is very low to produce correct thermodynamic model for the *KCpx* solid solution. However, existing experimental data allow the derivation of a simplified thermodynamic model for the system $CaMgSi_2O_6$–$KAlSi_2O_6$ for low K_2O concentrations.

Let us consider the equilibrium of *KCpx* with the alumino-silicate melt (L_{Si}) by taking into account the dependency of $K_p^{Cpx/L}$ on *P* and the SiO_2 content in the melt (Figs. 1 and 2). This equilibrium can be expressed as:

$$KAlSi_2O_6(KJd\ in\ CPx) = 1/4K_4Si_2O_6 + 3/4Al_{4/3}Si_2O_6(in\ L_{Si}), \quad (1)$$

The Gibbs free energy of this reaction is

$$\Delta G^0_{(1)} = \Delta H^0_{(1)} - T\Delta S^0_{(1)} + P\Delta V^0_{(1)} + RT\ln[(a^L_K)^{1/4}(a^L_{Al})^{3/4}/a^{Cpx}_{KJd}] \quad (2)$$

where $a_K{}^L$ and $a_{Al}{}^L$-activities of the $K_4Si_2O_6$ and $Al_{4/3}Si_2O_6$ components of the silicate melt, respectively; $L = L_{Si}$ and $a_{KJd}{}^{Cpx}$ is activity of the $KAlSi_2O_6$ component in the clinopyroxene solid solution; $\Delta G^0_{(1)}$, $\Delta H^0_{(1)}$, $\Delta S^0_{(1)}$ and $\Delta V^0_{(1)}$-free energy, enthalpy, entropy and volume differences for reaction (1).

Using the multi-site solution model, the mixing energy of the $K^{M2}Al^{M1}Si_2{}^TO_6$ (*KJd*) component in clinopyroxene is expressed as

$$RT\ln(a^{Cpx}_{KJd}) = RT(a^{id}_{KJd}) + G^e_{KJd} = RT[X^{M2}_K X^{M1}_{Al}(X^T_{Si})^2] + G^e_{KJd}, \quad (3a)$$

where X_i are mole fractions of components in corresponding sites and G^e_{KJd} — an excess free energy of the

Table 2
Available experimental data on compositions of *KCpx* and the alumino-silicate melt used in the regression

No.	Run No.	T (°C)	P (kbar)	Mineral assemblage	Compositional parameters							References
					KCpx				Melt			
					K^{M2}	Ca^{M2}	Na^{M2}	Al^{M1}	X_K	X_{Si}	X_{Al}	
1	1106	1600	110	*Ol + Grt + Cpx + X**	0.037	0.811	0	0.050	0.090	0.449	0.047	1
2	1163	1600	110	*Ol + Grt + Cpx*	0.046	0.804	0	0.053	0.065	0.504	0.044	1
3	1211	1550	90	*Cpx + Ol + Grt*	0.050	0.831	0	0.042	0.115	0.480	0.026	1
4	1212	1500	90	*Cpx + Ol + Grt*	0.037	0.846	0	0.041	0.118	0.419	0.129	1
5	1213	1550	75	*Cpx + Ol + Grt*	0.027	0.803	0	0.046	0.084	0.466	0.081	1
6	1208	1450	75	*Cpx + Ol + Grt*	0.027	0.862	0	0.034	0.131	0.414	0.118	1
7	1178	1500	50	*Cpx + Ol*	0.009	0.844	0	0.049	0.130	0.457	0.139	1
8	1179	1400	50	*Cpx + Ol*	0.011	0.834	0	0.059	0.121	0.459	0.128	1
9	–	1400	50	*Cpx + Grt + Cos*	0.014	0.446	0.337	0.570	0.085	0.619	0.139	2
10	–	1300	80	*Grt + Cpx + Cos + Rt + X**	0.046	0.513	0.214	0.244	0.207	0.545	0.080	3
11	–	1300	60	*Cpx + Grt + Cos + Phl + Ru*	0.062	0.531	0.017	0.308	0.138	0.600	0.083	4
12	–	1400	60	*Cpx + Grt + Cos*	0.0317	0.475	0.199	0.239	0.145	0.561	0.102	4
13	–	1500	60	*Cpx + Grt*	0.0278	0.452	0.191	0.246	0.138	0.531	0.105	4
14	–	1350	50	*Cpx + Grt*	0.0203	0.422	0.141	0.195	0.119	0.544	0.109	4
15	–	1300	50	*Cpx + Grt + Cos*	0.0277	0.403	0.146	0.197	0.106	0.546	0.109	4
16	–	1100	15	*Cpx*	0.0004	0.937	0.024	0.066	0.070	0.522	0.207	5
17	–	1100	20	*Cpx*	0.0004	0.904	0.042	0.132	0.053	0.535	0.216	5
18	–	1100	25	*Cpx*	0.0005	0.873	0.071	0.191	0.072	0.549	0.221	5
19	–	1200	25	*Cpx*	0.0004	0.894	0.046	0.105	0.071	0.559	0.232	5
20	P194	1200	30	*Cpx + Grt + Cos*	0.0005	0.532	0.333	0.509	0.035	0.679	0.175	6
21	S222	1400	50	*Cpx + Grt + Cos + Kfs*	0.011	0.513	0.329	0.522	0.036	0.696	0.179	6
22	S303	1900	100	*Cpx + Grt*	0.009	0.378	0.453	0.575	0.016	0.527	0.138	6
23	S257	1900	75	*Cpx + Grt*	0.009	0.411	0.344	0.576	0.021	0.522	0.150	6
24	S270	1700	60	*Cpx + Grt*	0.003	0.422	0.270	0.555	0.030	0.535	0.152	6
25	S228	1700	50	*Cpx*	0.002	0.478	0.238	0.455	0.020	0.500	0.158	6
26	P182	1500	30	*Cpx*	0.002	0.530	0.173	0.343	0.022	0.531	0.164	6

References: (1) Luth (1997), (2) Wang and Takahashi (1999), (3) Edgar and Mitchell (1997), (4) Edgar and Vukadinovic (1993), (5) Shimizu (1974), (6) Tsuruta and Takahashi (1998).
*X**—diverse K-bearing phases (Luth, 1995, 1997; Edgar and Mitchell, 1997).

KJd component in the clinopyroxene solid solution. G^{e}_{KJd} reflects a very limited solubility of *KJd* in clinopyroxene that corresponds to the strong non-ideality of the solid solution. In addition to the *Di*, *Hed*, *Jd* and *KJd* end-members, synthetic clinopyroxenes contain a significant amount of the *En–Fs* component (up to 20–30 mol%). Regarding the Mg-Fe-Ca-Na-K mixing in the M2 site, we tentatively used the five-member regular model for G^{e}_{Cpx} to derive G^{e}_{KJd}

$$G^{e}_{Cpx} = \sum_{i=1}^{c-1} \sum_{j\neq i}^{c} W_{ij} X_i X_j \tag{3b}$$

where $c = 5$; i, j–components in the M2 site (Mg, Fe, Ca, Na, K), and W_{ij}–interaction parameters, which could be computed by the regression of the experimental data.

Using similar approach, the mixing energy of the $K_4Si_2O_6$ component in the alumino-silicate melt is expressed as

$$RT\ln(a^{L}_{K}) = RT\left[(X^{L}_{K})^{4}\right] + (G^{e}_{K})^{L} \tag{3c}$$

and for the $Al_{4/3}Si_2O_6$ component

$$RT\ln(a^{L}_{Al}) = RT\left[(X^{L}_{Al})^{4/3}\right] + (G^{e}_{Al})^{L} \tag{3d}$$

Thus,

$$RT\ln\left[(a^{L}_{K})^{1/4}(a^{L}_{Al})^{3/4}\right) = RT\ln\left[(X^{L}_{K})(X^{L}_{Al})\right] + (G^{e})^{L} \tag{3e}$$

where X_i^L is mole fraction of *i*-component in the melt and $(G^e)^L$—a total excess free energy of the melt species, whose expression and parameters could be fitted by regression of the experimental data. The mole fraction of a component *i* in the melt is $X_i^L = i/(\mathrm{Si}+\mathrm{Ti}+\mathrm{Al}+\mathrm{Cr}+\mathrm{Fe}+\mathrm{Mn}+\mathrm{Mg}+\mathrm{Ca}+\mathrm{Na}+\mathrm{K})$, where symbols of elements denote their quantities in the melt formula per six oxygens. This approach allows the treatment of a wide range of the melt compositions (Table 2).

As a result, the best fit for 26 experimental data points (Table 2) at the least square error $r^2 = 0.934$ was obtained with the following values of Eq. (2):

$$\Delta H^0_{(1)} = -24317.3(\pm 6937)\ \mathrm{J/mol},$$

$$\Delta V^0_{(1)} = 0.219(\pm 0.106)\ \mathrm{J/mol/bar},$$

$$W_{\mathrm{Si}} = 1.716(\pm 0.5)\ \mathrm{J/mol/bar},$$

$$W_{\mathrm{KCa}} = 63881.44(\pm 9495)\ \mathrm{J/mol},$$

where W_{Si} is a parameter of the equation $(G^e)^L = W_{\mathrm{Si}}(X_{\mathrm{Si}}^L)^2 P(\mathrm{bar})$. $\Delta S^0_{(1)} = 0$ because of the independence of K_2O in *Cpx* on temperature (Mitchell, 1995; Luth, 1997; Edgar and Mitchell, 1997; Tsuruta and Takahashi, 1998). Influence of temperature on Eq. (2) through the compositional parameters is negligible. Testing of Eq. (3b) showed that in contrast to W_{KCa} an influence of other parameters from W_{ij} is also negligible, and we can omit them without loss of the accuracy.

Eq. (2) reproduces experimental pressure values and X_{K}^{Cpx} within ±9.1 kbar and ±0.012, respectively, in the intervals $T = 1100–1900$ °C and $P = 15–110$ kbar. The equation also illustrates the dependence of reaction (1) on *pressure*, *melt composition*, *and Cpx composition*. The positive value $\Delta V_{(1)}{}^0 =$

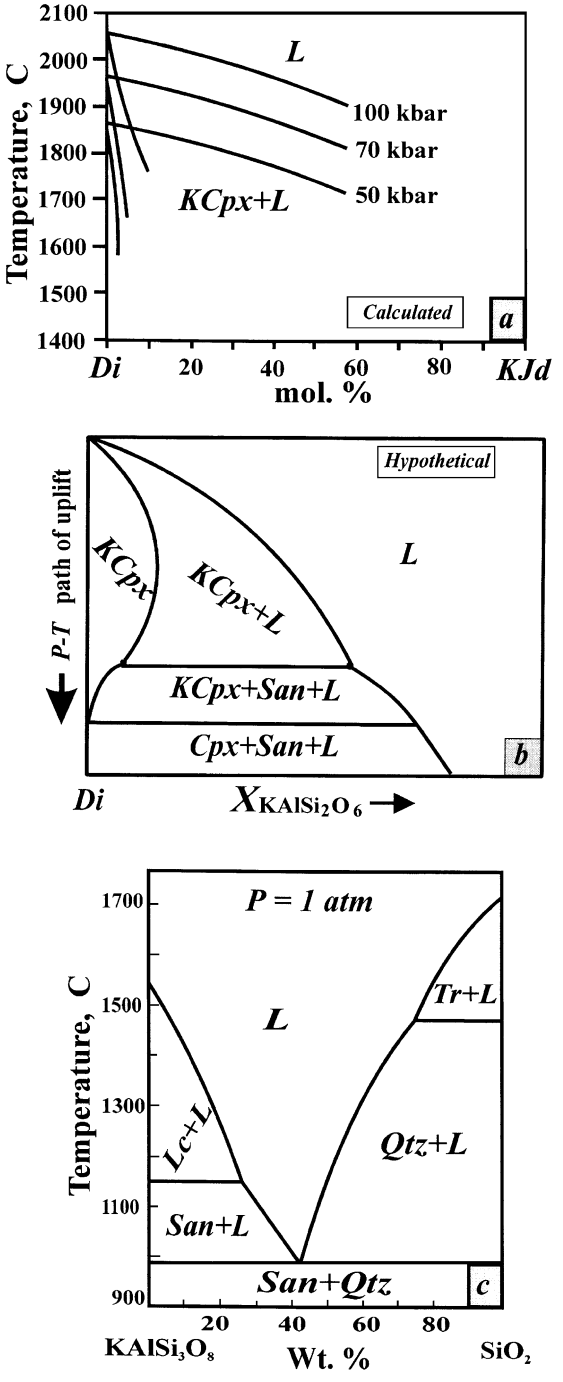

Fig. 3. Calculated (a) and hypothetical (b) diagrams for melting in the system *Di–KJd* and their comparison with the diagrams of melting in the systems $KAlSi_3O_8–SiO_2$ (diagram c, after Schairer and Bowen, 1955). The diagram (a) was calculated using Eq. (2) and data by Gasparik (1996) on diopside melting. Diagram (b) reflects change in phase relations with decrease of temperature taking into account that *P* and *T* form an uplift path (pseudo-isobaric diagram) and illustrates the possible existence of a peritectic point, similar to that in the system $KAlSi_3O_8–SiO_2$ (diagram c).

0.219 ($\pm$0.106) J/mol/bar reflects the observed dependence of the potassium content in *Cpx* in equilibrium with the alumino-silicate melt on pressure. Compositional factors can amplify or moderate this effect without change of its sign. The calculated $W_{Si} = 1.716(\pm 0.498)*P$(bar) J/mol reflects the observed positive correlation of K_2O in clinopyroxene with SiO_2 in coexisting melt (Fig. 2a,b). Fig. 2c shows some dependence of K_2O in *Cpx* on Al_2O_3 in the coexisting melt. However, in contrast to SiO_2, Al_2O_3 in the melt strongly correlates with pressure and, therefore, concentration of Al_2O_3 in the melt is already regarded in Eq. (2). Eq. (3b) shows that addition of any component (i.e., *Jd*, *En*, *Fs*) into the *Di*(*Hed*)–*KJd* solid solution results in decrease of the potassium solubility in clinopyroxene, as well.

We used Eq. (2) and the data by Gasparik (1996) on diopside melting for calculation of the high-temperature isobaric relation in the system *Di*–*KJd*, which is a portion of the system *Di*–*Kfs*. Fig. 3a illustrates the major features of the *KCpx*–liquid equilibria. Low-$KAlSi_2O_6$ clinopyroxene precipitates first from a melt at high temperature. It becomes richer in the *KJd* component with decrease of temperature at any pressure. However, solubility of the *KJd* component in clinopyroxene drastically drops with decrease of pressure. As pressure decreases, both clinopyroxene and liquid compositions displace toward the alkali-poor region of the system. By now, there are no data on *KCpx* equilibria at temperatures below 1600–1500 °C. However, we assume that there should be a "pseudo-peritectic" point at pressures below 60–50 kbar which produces K-feldspar and potassium-free clinopyroxene (Fig. 3b). This conclusion follows from both the experimental and natural data. Experiments by Mitchell (1995), Tsuruta and Takahashi (1998) and Wang and Takahashi (1999) show that the potassium content of clinopyroxene abruptly drops (by 0.5–1 wt.%) in presence of K-feldspar. Similar conclusion has been done from the study of K-feldspar blebs in clinopyroxene from garnet–clinopyroxene rocks of the Kokchetav Complex (see below, Perchuk et al., 1996). The proposed peritectic reaction is analogous to the reaction of an incongruent melting of sanidine in the system *San*–*Qtz* at $P = 1$ atm (Fig. 3c, Schairer and Bowen, 1955).

5. Immiscibility in the carbonate–silicate melts and the stability of *KCpx*

Liquid immiscibility in sodic carbonate–silicate systems was experimentally investigated (Koster van Groos and Wyllie, 1968, 1969, 1973; Freestone and Hamilton, 1980; Perchuk and Lindsley, 1982; Lee and Wyllie, 1997, 1998; Wyllie and Lee, 1998), following the discovery of sodic carbonatitic lavas (e.g., Dawson et al., 1987; Dawson, 1989) and sodic carbonate inclusions in minerals from alkalic rocks (e.g., Kogarko et al., 1991; Solovova et al., 1996; Nielsen et al., 1997). Freestone and Hamilton (1980) found that a miscibility gap in the system SiO_2-Al_2O_3-TiO_2-CaO-FeO-MgO-Na_2CO_3-H_2O at 1250 °C expands with the increase of P from 2 to 7.6 kbar, mostly at expense of displacing of the field of the silicate melt toward the alkali-poor region. This conclusion has been experimentally tested by Wyllie and Lee (1998) in the pseudo-ternary system [SiO_2, Al_2O_3]-Na_2O-(Ca,Mg,Fe)O. Wyllie and Lee (1998) found, however, complete miscibility at $P > 25$ kbar and 1300–1500 °C (se also Lee and Wyllie, 1998). Fig. 4 demonstrates systematic decrease of the silicate melt field with the increase of P or the decrease of Al/Si ratio in the melt.

Carbonatites often accompany alkali-rich basic and ultra-basic magmatism in continental platforms, but only locally in oceanic islands (e.g., Tenerife). This observation has been explained by a model of carbonation of basaltic magmas (Perchuk, 1971), whereby an increase of the Na_2O and CO_2 activities in deep-seated fluid drives the reaction:

$$\begin{aligned} &NaAlSi_3O_8(Ab) + CaFeSi_2O_6(Hed) \\ &\quad + (1.5Na_2O + CO_2)_{fluid} \\ &\quad = 2NaAlSiO_4(Ne) + NaFeSi_2O_6(Aeg) \\ &\qquad + 2CaCO_3(Cal). \end{aligned} \tag{4}$$

to the right. Owing to carbonate–silicate liquid immiscibility, the increase of Na_2O and CO_2 activities leads to the formation of the association *ijolite* (*Ne*+*Aeg*)+*carbonatite* (*Cal*) instead of the usual basalt or gabbro (*Pl*+*Hed*). An experimental study of the system $NaAlS_3O_8$-$CaAl_2Si_2O_8$-Na_2CO_3-H_2O

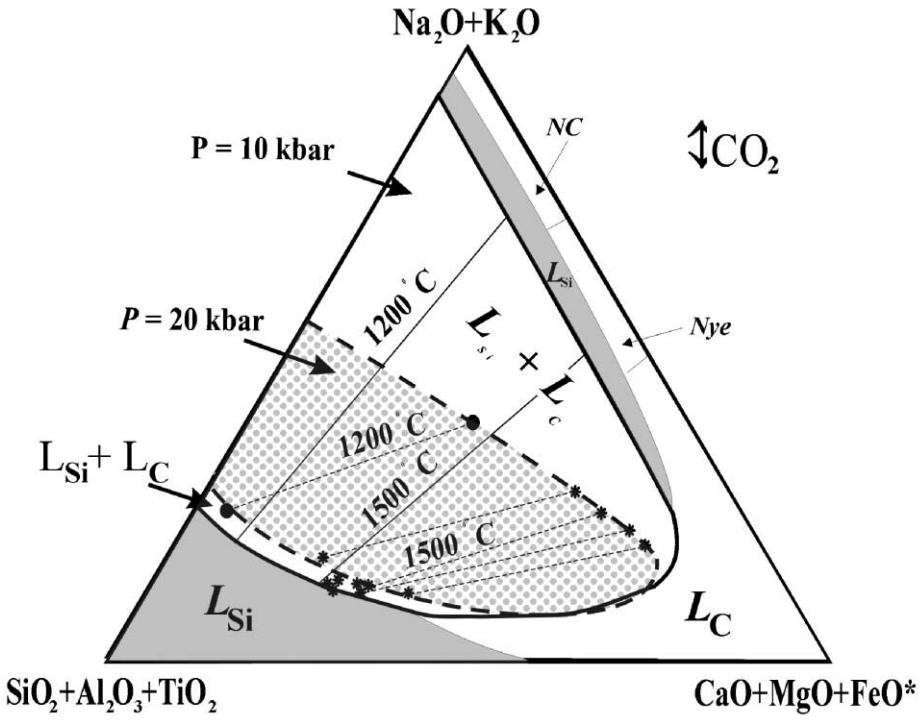

Fig. 4. Melting relations for the pseudo-ternary system $[SiO_2$-Al_2O_3-$TiO_2]$-(Ca,Fe,Mg)O-$(K,Na)_2CO_3$ (of the Freestone and Hamilton's, 1980 projection from the CO_2 apex) illustrating the immiscibility of carbonate–silicate liquid in the sodic system at 10 kbar (solid) and in the potassic system at 20 kbar (dashed). $P=10$ kbar. The system SiO_2-Al_2O3-CaO-Na_2CO_3 (Lee and Wyllie, 1998); tie-line 1200 °C corresponds to the same system at $P=20$ kbar in the presence of H_2O (Perchuk and Lindsley, 1980a, 1982). $P=20$ kbar. The system $[SiO_2$-$Al_2O_3]$-(Ca, Mg)O-K_2CO_3, showing carbonation of garnet peridotite melt at $T=1500$ °C in the presence of H_2O (Perchuk and Lindsley, 1980a,b, 1982). A strong effect of P on the mutual solubility of silicate melt and carbonate liquid and, consequently, an abrupt widening of the miscibility gap toward alkali-rich melts (see text) is apparent. *Nye*—nyerereite stability field (Lee and Wyllie, 1998).

(Koster van Groos and Wyllie, 1973) confirmed the immiscibility of carbonate and silicate melts. Later, Perchuk and Lindsley (1982) studied reaction (4) in the system $NaAlS_3O_8$-$CaAl_2Si_2O_8$-Na_2CO_3-K_2CO_3-$CaCO_3$-H_2O using plagioclase glasses of compositions $An_{90}Ab_{10}$ and $An_{90}Ab_{10}$ (in mol%) at 10 and 20 kbar and 1200–1500 °C. Alkali and CO_2 activities were fixed by Na, K and hydrate salts, as well as by $C_2H_4O_4{\cdot}2H_2O$ and $C_3H_4(OH){\cdot}3Na_2CO_3{\cdot}5H_2O$. The experiments showed that the melt split into two silicate liquids and one carbonate–silicate liquid. The shaded area in Fig. 4 denotes the L_{Si}–L_c miscibility gap at 20 kbar in the potassic system. Compositions of the carbonate–silicate liquid were calculated on the basis of the compositions of a starting mixture and the silicate melt after the experiment (Perchuk and Lindsley, 1982). The slopes of the tie-lines are gentler in comparison with the sodic system. That indicates that the silicate melt depleted in alkalis can coexist with potassium salt melts (K_2CO_2 or KCl), whereas the potassium partition coefficient for the two liquids must be larger than 20 in favor of the salt melt. In this case, a high potassium activity is buffered in the silicate melt by the coexisting salt melt and may provide the conditions for the crystallization of *KCpx* from the silicate melt.

Koster van Groos and Wyllie (1973), Lee and Wyllie (1997, 1998), Wyllie and Lee (1998) as well as Freestone and Hamilton (1980) not only confirmed the immiscibility in the Na–Ca–carbonate–silicate systems, but also provided phase diagrams.

In contrast, the system K_2O-CaO-SiO_2-Al_2O_3-CO_2 was not studied systematically. The nature and the behavior of ultra-potassic salt melts at high *P* has been studied only superficially. Perchuk and Lindsley (1982) studied the carbonation of garnet peridotite melt in the system $Mg_3Al_2Si_3O_{12}$-$CaMgSi_2O_6$-K_2CO_3-H_2O at 1500 °C and 20 kbar in order to find evidence for the carbonate–silicate immiscibility. Glass globules of phlogopite composition included in Ca–Mg–K carbonate matrix were found after the experiments. As expected, the carbonate fraction extracted Ca and partially Mg from the silicate melt (Fig. 4). Other information on immiscibility of potassium-rich alumosilicate and carbonate–silicate melts is very restricted and non-systematic. Harlow (1997) observed rare silicate globules in the experiments on potassium exchange between K_2CO_3 melt and *KCpx* at 100 kbar. However, Matveev et al. (1998) did not observe such carbonate–silicate immiscibility in the system $K_2Mg(CO_3)_2$-K_2CO_3-*Di-Grs* at 70 kbar and 1500–1600 °C.

Besides the preliminary study of Perchuk and Lindsley (1982), liquid immiscibility in potassic carbonate–silicate systems has not been studied experimentally. Perchuk and Yapaskurt (1998) suggested that the observation of Freestone and Hamilton (1980) can be applied for potassic systems: the miscibility gap abruptly narrows and moves to the alkali-poor region with the increase of pressure. Therefore the increase of pressure expands the field of the potassic carbonate liquid and contracts that of the silicate liquid.

The above review shows that the most experimental studies of the carbonate–silicate systems were carried out to solve the problem of genesis of carbonatites. From mid-1990s, Jones et al. (1995), Litvin et al. (1997), Pal'yanov et al. (1998, 1999), Sokol et al. (1998, 2000) and Borzdov et al. (1999) showed that the alkali-carbonate and the alkali-carbonate–silicate systems are appropriated media for synthesis of large diamond crystals. In addition, investigations of phase relationships in the potassium-bearing carbonic-alumino-silicate systems seems to be the right way to understanding the origin of ultra-high pressure rocks with diamond, *KCpx*, phlogopite, etc.

6. A review of the natural data

6.1. Inclusions of KCpx in diamonds and garnets

There are numerous reported occurrences of *KCpx* as inclusions in diamonds from eclogite and peridotite nodules in kimberlites and lamproites (e.g., McGregor and Carter, 1970; Moore and Gurney, 1985; Ricard et al., 1989; Harlow and Veblen, 1991; Stachel et al., 2000). Prinz et al. (1975) pointed out a wide variation of K_2O in *Cpx* inclusions in diamonds (0.02–0.87 wt.%). Reid et al. (1976) found up to 0.29 wt.% of K_2O in *Cpx* from diamondiferous eclogites. Having summarized all known data on *Cpx* composition from mantle xenoliths and inclusions in diamonds, Bishop et al. (1978) showed that *Cpx* from eclogites was richer in potassium, than *Cpx* from lherzolites. The K_2O content in *Cpx* from eclogites varies from 0.05 to 1.62 wt.%, whereas it is less then 0.37 wt.% in lherzolites. Based on the correlation of Na_2O in garnet with K_2O in coexisting *Cpx*, Bishop et al. (1978) confirmed strong dependence of the K_2O content in *Cpx* on pressure. Stachel et al. (2000) described *KCpx* (0.53–1.44 wt.% K_2O) coexisting with Na_2O-bearing majoritic garnets (6.313–6.558 Si atoms in garnet formula per 24 oxygen) from inclusions in diamonds from the Kankan region (Guinea). All these data unambiguously proved the ultra-high pressure origin of natural *KCpx*.

Perchuk et al. (1996) reported about 1.2 wt.% K_2O in *Cpx* from diamond-free coarse-grained garnet-clinopyroxene silicate rocks (Group A) of the Kumdy-Kol microdiamond mine in the Kokchetav Complex, Kazakhstan. Even higher content of K_2O, up to 1.5 wt.%, was measured in *Cpx* from garnet-clinopyroxene fine-grained carbonate–silicate rocks (Group B) (Sobolev and Shatsky, 1990; Perchuk et al., 1995; Shatsky et al., 1999). Average chemical compositions of the rock groups are:

	SiO_2	TiO_2	Al_2O_3	Cr_2O_3	FeO	MgO	CaO	Na_2O	K_2O	P_2O_5	CO_2
A	54.7	0.23	8.44	0.08	4.17	11.80	16.02	4.02	0.12	0.25	4.65
B	56.4	0.24	8.84	0.12	3.51	9.88	13.35	2.16	1.81	0.26	21.78

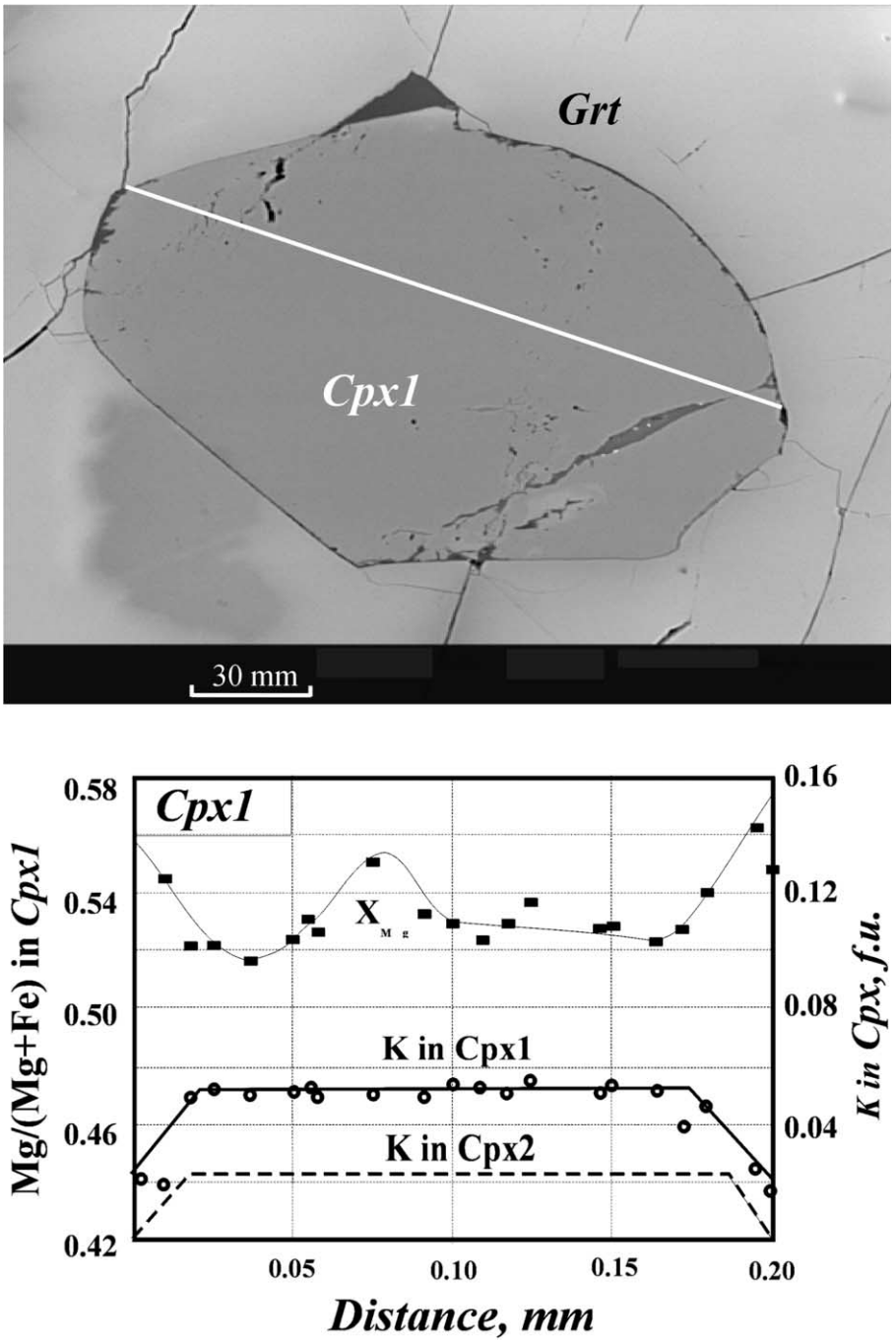

Fig. 5. A back-scattered electron image of an inclusion of *KCpx* (*Cpx*1) in *Grt* grain from pyroxene–garnet rock (Group A, see text) of the Kumdy-Kol mine in the Kokchetav Complex (N. Kazakhstan) and a microprobe profile (solid) across this grain (Perchuk et al., 1996; Perchuk and Yapaskurt, 1998). The profile of the potassium content in matrix *Cpx* (*Cpx*2) containing *Kfs* blebs from Fig. 6 is shown for comparison (dashed). Electron microscope CamScan.

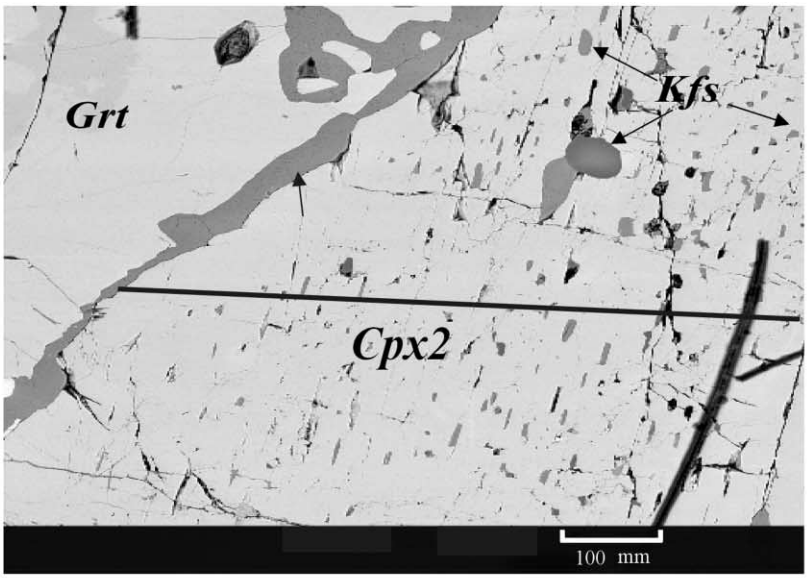

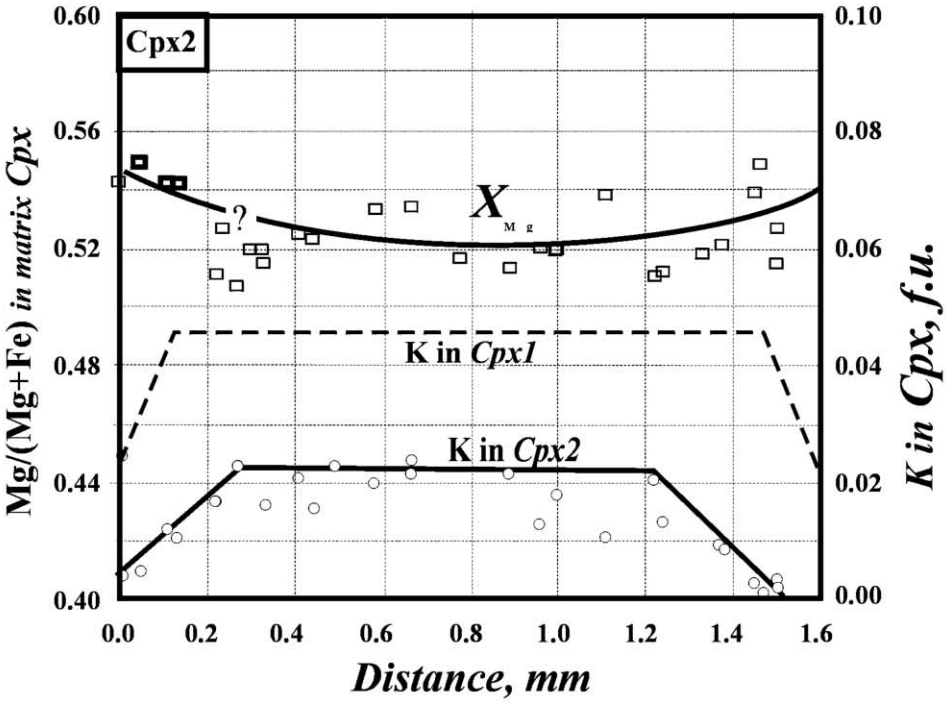

Fig. 6. A back-scattered electron image of the matrix *Cpx* (*Cpx*2) with *Kfs* blebs in the core from the diamond-free K-poor pyroxene–garnet rock (Group A, see text) of the Kumdy-Kol mine in the Kokchetav Complex (N. Kazakhstan) and a microprobe profile across this grain. The analyses are made with defocused beam in order to obtain an integrated bulk composition in every point (Perchuk et al., 1995; Perchuk and Yapaskurt, 1998). The profile of the potassium content in *Cpx*1 inclusion in garnet from Fig. 5 is shown for comparison. Electron microscope CamScan.

These undeformed rocks form interlayers, boudins, and lenses in strongly foliated garnet-biotite diamondiferous gneisses and schists and alternate with the eclogite boudins (Lavrova et al., 1999). The relationships of *KCpx*, potassium-free clinopyroxenes, and *Kfs* in the rocks of Group A are the most interesting. The rocks are composed of large (locally up to 7 cm) grains of garnet and clinopyroxene, accessory sphene, apatite, calcite, and secondary quartz, hornblende, K-feldspar, epidote, and calcite (Perchuk et al., 1995, 1996). Garnet contains microinclusions of *KCpx* (*Cpx*1) whose K_2O concentrations can reach 1.2 wt.% (see the top of Fig. 5). The bottom of Fig. 5 illustrates the distribution of potassium (f.u.) and X_{Mg} across a ~ 200 μm wide inclusion of *KCpx* in the *Grt*. The K_2O content in the core of the *Cpx*1 inclusion is uniform. At its edges, K_2O symmetrically drops from 0.055 (~ 1.2 wt.%) to 0.02 f.u. (~ 0.4 wt.%). The X_{Mg} profile is more complicated. According to Perchuk and Yapaskurt (1998), it reflects a sequence of mineral precipitation from a melt during uplift and cooling. Being the liquidus mineral, *Cpx*1 precipitated first (X_{Mg} decreases), and subsequently *Grt* forms (X_{Mg} increases) at lower *T* and *P*. The cores of large matrix *Cpx* in the rocks (*Cpx*2) contain tiny, less then 10 μm, *Kfs* blebs (Fig. 6). The bottom of Fig. 6 shows a compositional profile across *Cpx*2 obtained with a defocused electron beam. Similar to *Cpx*1, the integrated K_2O content in core in *Cpx*2 is constant, about 0.02 f.u., but symmetrically decreases to zero in the rims (Perchuk et al., 1995; Perchuk and Yapaskurt, 1998). Reid et al. (1976) described similar *Kfs* blebs in potassium-free *Cpx* in diamondiferous eclogite from African kimberlite pipes (South Africa, Botswana, Tanzania). The sodium content in *Grt* from these eclogites reached 0.15 wt.% and is positively correlated with Ti (substitution *Grs*-Na $Ca_2[Ti,Al]Si_3O_{12}$). The jadeite content in coexisting *Cpx* varies from 20 to 60 mol%. Taking this into account, Reid et al. (1976) suggested that the crystallization of *Grt* and *Cpx* from a melt occurred at a depth of about 180–200 km. A subsequent uplift of eclogite toward the Earth's surface caused the exsolution of jadeite from *Cpx*. Partial melting of the rock during the rapid uplift led to K_2O partitioning into the melt, which was subsequently preserved as the *Kfs* blebs in *Cpx*. Luth (1997) proposed that the

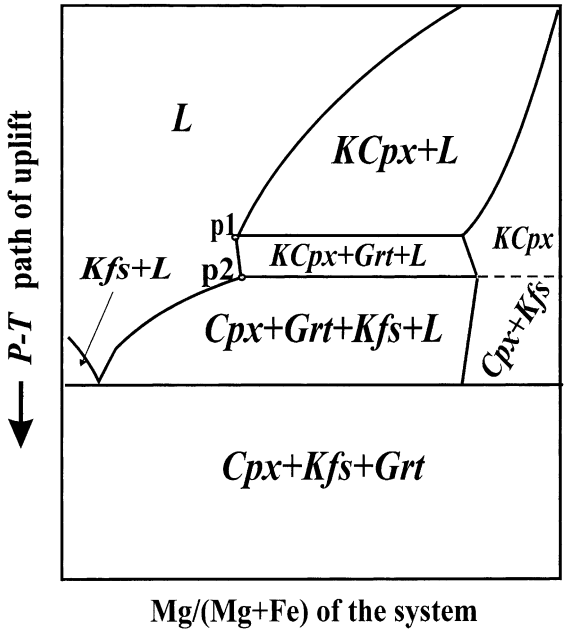

Fig. 7. Hypothetical pseudo-isobaric $T–X$ ($X=X_{Mg}=Mg/Mg+Fe$) diagram of melting for the pseudobinary system *Grt–KCpx*, deduced from relationships between *Cpx*1, *Cpx*2, *Grt*, and *Kfs* and their compositions and zoning, shown in Figs. 5 and 6 (after Perchuk and Yapaskurt, 1998).

formation of blebs is related to exsolution from *Cpx* by the reaction:

$$3KAlSi_2O_6 + 2Ca_{0.5}AlSi_2O_6 = 3KAlSi_3O_8 + CaAl_2SiO_6, \quad (5)$$

or

$$KCpx + Esk = Kfs + Tsc.$$

In contrast, *KCpx* (*Cpx*1) from clinopyroxene–garnet rocks of the Kokchetav Complex does not contain the Ca-eskolaite end-member. Therefore, reaction (5) is unable to explain the formation of the *Kfs* blebs in *Cpx*2 (Perchuk et al., 1995, 1996). On the basis of phase relationships and chemical zoning of both the *Cpx*1 inclusions in *Grt* and the matrix *Cpx*2 with the *Kfs* blebs (Fig. 6) from the pyroxene–garnet rocks of Group (A), Perchuk and Yapaskurt (1998) showed that reaction (6)

$$KAlSi_2O_6 + [SiO_2]_{melt} \Rightarrow KAlSi_3O_8, \quad (6)$$

or

$$KJd\ (\text{in } Cpx) + [SiO_2]_{melt} = Kfs,$$

operates during uplift and cooling of the potassium-rich carbonate–silicate melt. In addition to Fig. 3b illustrating peritectic point in the system diopside-sanidine, Fig. 7 demonstrates hypothetical non-isobaric *TX* ($X = X_{Mg} = Mg/Mg + Fe$) diagram of melting for pseudobinary system *Grt–KCpx* deduced from the data of detailed microprobe profiles of *Cpx*1 (Fig. 5) and *Cpx*2 (Fig. 6) from the Kokchetav *Grt–Cpx* rocks.

6.2. Non-crystalline inclusions in diamonds

In order to determine the source and the depth of melt generation and its primary composition, the most useful information can be obtained from analyses of non-crystalline inclusions in minerals from carbonatites and in diamonds from kimberlite and lamproite pipes. Despite the successful experiments on diamond crystallization in alkali or alkali-earth carbonate and carbonate–silicate systems (Jones et al., 1995; Litvin et al., 1997; Pal'yanov et al., 1998, 1999; Sokol et al., 1998, 2000; Borzdov et al., 1999), analysis of fluid and melt inclusions in minerals from carbonatites (e.g., Kogarko et al., 1991; Solovova et al., 1996; Nielsen et al., 1997) does not support deep-seated origin of majority of carbonatitic melts. The absence of diamond in carbonatites, even as inclusions in phenocrysts, indicates a relatively shallow depth of their origin, i.e., less then 100 km. Nevertheless, diamonds are common in kimberlites and lamproites. It is now evident that diamonds from kimberlites and lamproites contain inclusions of mantle minerals, fluids, silicate melts and brines. Non-crystalline inclusions in diamonds (Dawson et al., 1987; Navon et al., 1988;

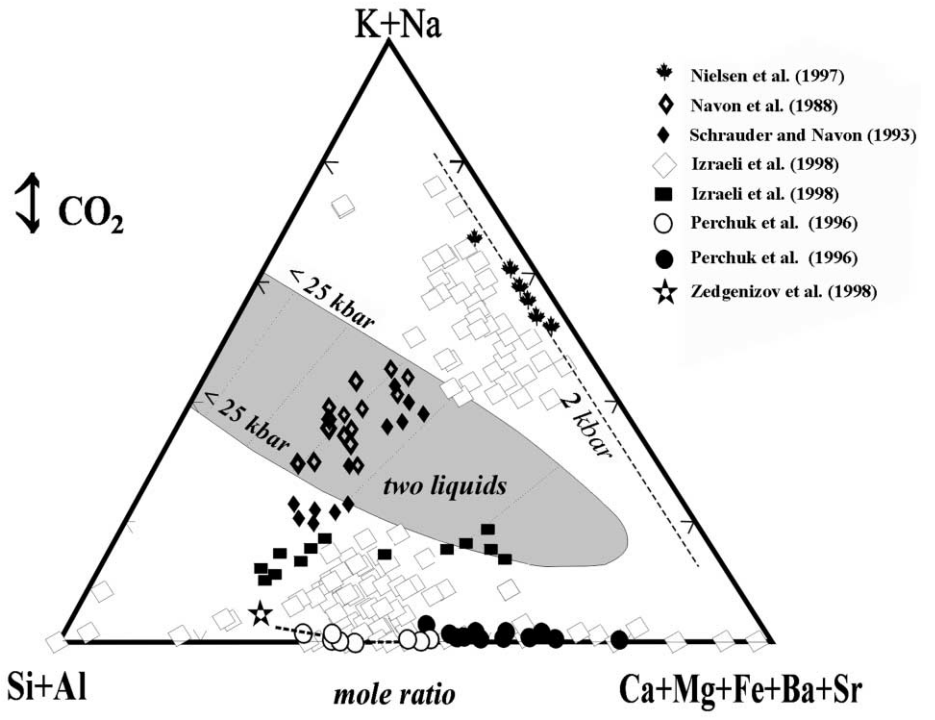

Fig. 8. The Freestone and Hamilton's (1980) projection from $CO_2 + Cl$ apex showing a comparison of the compositions of fluid inclusions in diamonds (all open and solid diamonds and rectangles) from some African kimberlite pipes with the composition of some fluid inclusions in carbonatites (maples), bulk compositions of *Grt–Cpx* (open circles) and calc-silicate rocks (solid circles) from the Kokochetav complex (Kazakhstan). Asteriks represent the composition of the silicate melt from Fig. 10. See text for further explanation.

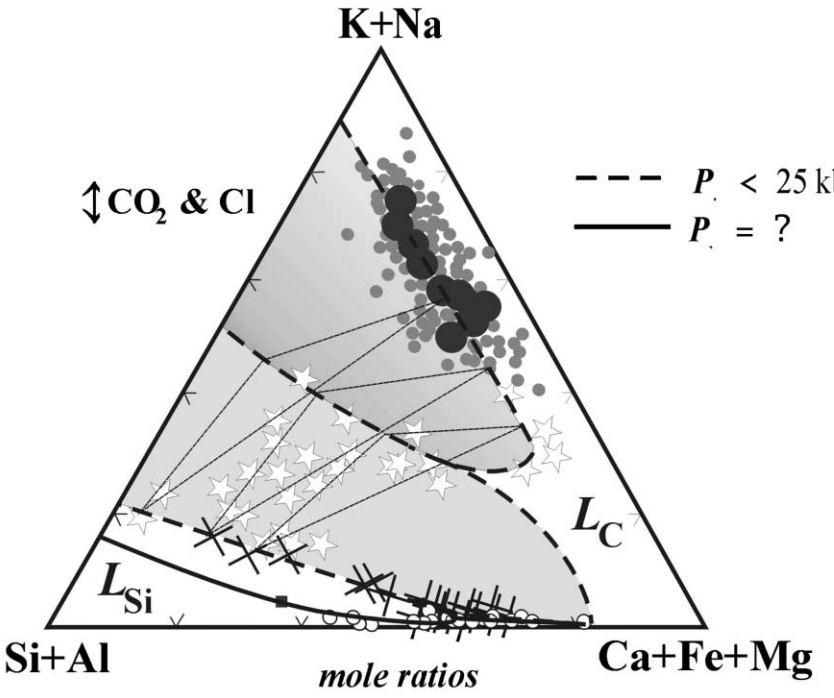

Fig. 9. Plot of fluid (open and solid rhombs) and brine compositions from inclusions in diamonds, some kimberlites and lamproites onto the Freestone and Hamilton's (1980) projection from CO_2. Large solid diamonds—Brines: black circles—average compositions of the brine in the nine diamonds, small gray circles-analyses of the individual inclusions in all nine diamonds. Stars—average compositions of fluid inclusions in fibrous diamonds. Crosses—lamproites, xs—kimberlites. Solid rectangle = asterisk from Fig. 8, open circles = silicate and calc-silicate magmatic rocks from Kumdy-Kol microdiamond main, the Kockchetav complex (northern Kazakhstan).

Dawson, 1989; Chen et al., 1992; Schrauder and Navon, 1993, 1994; Schrauder et al., 1993, 1996; De Corte et al., 1998; Izraeli et al., 1998, 1999, 2001; Zedgenizov et al., 1998; Navon, 1999; Navon and Izraeli, 1999) indicate pressure of their entrapment of about 40–70 kbar (e.g., Navon, 1991), i.e., to a depths interval from 120 to 200 km.

6.3. Fluid inclusions in diamonds

Very few data exist on composition of fluid inclusions in diamond because of detection and analytical problems. According to Navon et al. (1988), Chen et al. (1992) and Izraeli et al. (2001), only three major groups of fluid inclusions are present in diamond: (1) silicate-bearing of diverse composition; (2) aqueous-carbonic fluid and (3) brine. However, because of their small size, measurements on such inclusions are imprecise and some analyses correspond to mixtures of inclusions. In Fig. 8, a portion of the fluid-melt inclusions (open and solid diamonds) corresponds approximately to equal mixtures of all three constituents (Navon, personal communication). The diagram also shows a preliminary two-phase immiscibility region of the fluidized silicate melt in absence of the salt melt presumably at pressure of above 20–25 kbar and T>1000 °C. All inclusions are characterized by K/Na $\gg$ 1 as exemplified by the data (wt.%) from Navon et al. (1988) and Schrauder and Navon (1994):

#	1	2	3	4	5	6	7	8	9	10	11	12	13
Na_2O	2.4	2.6	2.2	3.0	2.3	3.5	3.8	3	2.9	2.3	2.4	2.7	3.4
K_2O	18.7	21.4	22.2	18.4	18.1	29.7	17.7	23.7	20.8	19.4	21.1	25.2	19.3

This large K/Na ratio is able to explain coexistence of diamond with *KCpx* rather than omphacite. De Corte et al. (1998) showed that microdiamonds from metamorphic rocks of the Kokchetav massif are similar to those of kimberlitic pipes. On the other hand, analyzing the infrared spectra of microinclusions in microdiamonds from garnet grains of the rocks, De Corte et al. (1998) observed predominance of the aqueous inclusions containing solid carbonate minerals. That indicates a high oxygen fugacity in the C–O–H fluid during the diamond formation.

6.4. Brine inclusions in diamond

Chen et al. (1992) was the first to report an occurrence of concentrated KCl inclusions in diamond. Similar inclusions were subsequently found in diamonds from kimberlite pipes Koidu (Sierra-Leone), Koffiefontein (South Africa) and Udachnaya (Russia) (Fig. 9; Navon and Izraeli, 1999; Izraeli et al., 1999, 2001). The average composition of the brine from these inclusions is (wt.%): 30–40 H_2O, 30–34 (Na,K)Cl, 23–25 (Fe,Ca,Mg)CO_3, 3–4 SiO_2 and 5% of an undetected chloride (to account for the systematic excess of the observed chlorine). Izraeli et al. (2001) suggested an average formula for this fluid: $(K,Na)_8(Ca,Fe,Mg)_4SiO(CO_3)_4Cl_{10}(H_2O)_{28-44}$. They assumed that the fluid inclusions were mixtures of two fluids, i.e., a KCl–NaCl brine and a Ca, Na, Si, Fe, Mg-rich carbonate fluid. This conclusion is supported by the direct correlation of the alkali-earth component with $X^{fl}_{CO_2}$.

6.5. Inclusions of silicate melt in diamond

Navon et al. (1988), Schrauder and Navon (1994), and Izraeli et al. (2001) investigated silicate melt inclusions in diamond from kimberlites of Botswana and Zair (Table 3). The major characteristics of the melt inclusions are very low aluminum contents ($Al_2O_3 < 6$

Table 3
Selected analyses on metallic oxides, and H_2O/CO_2 ratios in fluid inclusions trapped by diamonds (Navon et al., 1988; Schrauder and Navon, 1994)

Sample #	JWN 110	CTP 6268	JWN 108	JWN 106	JWN 89	CTP LB	CTP MM1	CTP L0	CTP L6	GRR 1504	GRR 1508	GRR 1517	GRR 1518
Region	**Botswana**					**Zair**				**No data**			
Points*	42	4	70	16	27	2	2	5	2	8	10	3	2
SiO_2	41.3	31.9	23.9	28.4	29.4	34.6	40.4	41.2	43.3	42.3	42.4	30.3	42.4
TiO_2	4.6	4.2	4.6	4.9	4.8	2.1	2.9	2.4	2.5	2.6	2.7	3.4	2.9
Al_2O_3	4.9	2.9	2.5	2.2	2.9	5.6	4.5	6.1	5.4	4.9	4.9	5.3	4.4
FeO	11.1	15.7	15.2	14.9	16.1	4.9	7.2	5	5.6	11.1	6.1	5	8
MgO	5.1	5.7	10.9	10.6	8.2	2.3	4.6	2.8	3.8	4.6	3.6	4.3	4.9
CaO	6.8	10.5	13.5	12.6	13.4	12.3	13.9	10.7	10.6	7.8	11.9	18.7	9.8
Na_2O	2.4	2.6	2.2	3.0	2.3	3.5	3.8	3	2.9	2.3	2.4	2.7	3.4
K_2O	**18.7**	**21.4**	**22.2**	**18.4**	**18.1**	**29.7**	**17.7**	**23.7**	**20.8**	**19.4**	**21.1**	**25.2**	**19.3**
Total**	94.9	94.9	95.0	95.0	95.2	95.0	95.0	94.9	94.9	95.0	95.0	94.9	95.1
H_2O, ppm	64	407	99	38	128	140	165	191	619	118	269	241	115
CO_2, ppm	120	600	250	75	420	66	89	79	135	44	133	139	70
$X^{fl}_{H_2O}$ ***	0.6	0.5	0.5	0.6	0.4	0.8	0.6	0.8	0.8	0.8	0.7	0.8	0.8

* Number of inclusion analyses for each diamond crystal.

** Average major oxide compositions (wt.%) of the volatile-free fractions of the inclusions, normalized to the sum of eight rock-forming oxides equal to 95%.

*** $X^{fl}_{H_2O} = H_2O/H_2O + CO_2$, molar fraction of H_2O in a fluid.

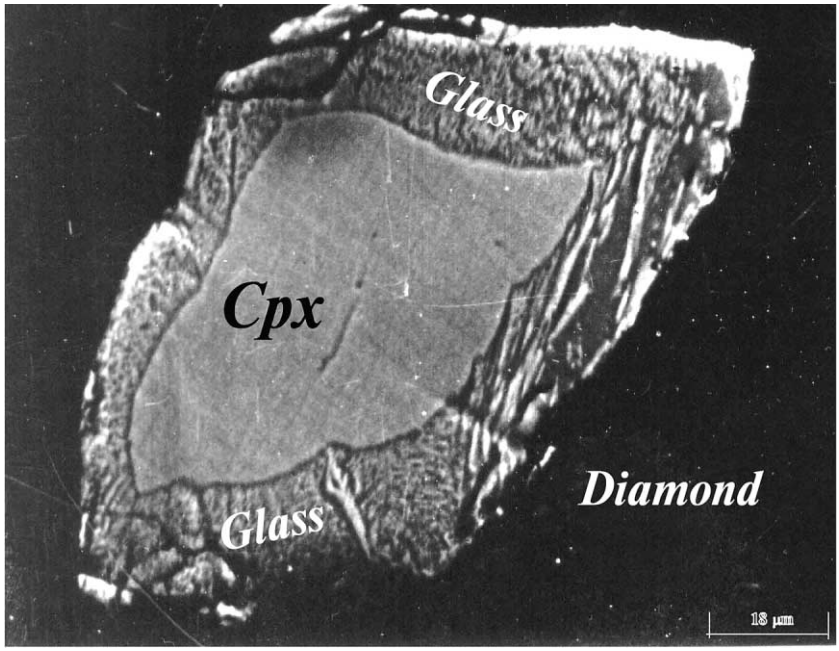

Fig. 10. Omphacite grain surrounded by a silicate glassy matrix; an inclusion in diamond from the Satykanskaya kimberlite pipe, Yakutia (Zedgenizov et al., 1998). *P* of 81–83 kbar for 1000–1800 °C was calculated with Eq. (2).

wt.%), wide variations of SiO_2 content (from 24 to 58 wt.%), and high alkalinity with significant predominance of potassium over sodium. The following nine examples (wt.%) clearly illustrate the conclusions of Izraeli et al. (2001) on extremely potassic fluid:

	1	2	3	4	5	6	7	8	9
Na_2O	4.6 ± 2.7	1.9 ± 2.4	1.1 ± 1.2	9.9 ± 6.9	4.4 ± 1.8	2.8 ± 4.3	2.5 ± 0.8	2 ± 0.9	3.7 ± 2.6
K_2O	28.8 ± 4.9	31.9 ± 3.4	36.5 ± 1.3	29.8 ± 1.8	26.7 ± 3.2	39 ± 5.7	33.7 ± 4.2	30.6 ± 4.2	31.4 ± 4.4
K_2O/Na_2O	6.26 ± 1.81	16.8 ± 1.4	33.2 ± 1.2	3 ± 0.26	6,07 ± 1.8	13.9 ± 1.3	13.5 ± 5.2	15.3 ± 4.7	8.5 ± 1.7

The studied inclusions are also characterized by relatively low X_{CO_2} ($CO_2/(H_2O+CO_2)$) that varies from 10 to 50 mol% (Navon et al., 1988; Schrauder and Navon, 1994). The Ca, Mg and Fe contents in the inclusions correlate directly with CO_2. The aqueous inclusions are richer in Al_2O_3 and SiO_2, while the carbonate inclusions are enriched in alkali, alkali-earth components, and P_2O_5. Elevated concentrations of chlorine are also evident.

Data on inclusions in diamonds from kimberlite pipes from Sierra-Leone, South Africa and Yakutia (Izraeli et al., 2001) indicate that the inclusions of silicate melt are accompanied by the inclusions of highly concentrated KCl brines and diverse mineral inclusions. Mineral inclusions, associated with the ultra-potassic melts and fluids, belong to either eclogite (*Grt–Cpx*) or peridotite (*Grt–Cpx–Ol*) assemblages.

Zedgenizov et al. (1998) published data on a potassic-bearing clinopyroxene included in diamond from the Satykanskaya kimberlitic pipe. The core of this inclusion composed of *KCpx* is surrounded by glass (solidified fluidized silicate melt) (Fig. 10). The compositions of these phases are the following:

	SiO_2	TiO_2	Al_2O_3	Cr_2O_3	MnO	FeO	MgO	CaO	Na_2O	K_2O
KCpx	54.7	0.23	8.44	0.08	0.06	4.17	11.8	16.02	4.02	0.12
Melt (?)	56.4	0.24	8.84	0.12	0.01	3.51	9.88	13.35	2.16	1.81

The presence of such inclusion implies crystallization of *KCpx* within the diamond field stability. Despite the very low K_2O contents in the inclusion, the melt is by 15 times richer in potassium than the coexisting pyroxene. These data allows estimation of pressure for *KCpx* crystallization using Eq. (2): $P = 81-83$ kbar within the wide temperature interval, from 1000 to 1800 °C. These values correspond to the depth of about 250 km.

Thus, the available data suggest that in the upper mantle, at ~40–50 kbar and ~1100–1500 °C, minerals can coexist with three liquid phases: aqueous-carbonic fluid, silicate melt and brine. Immiscibility in the carbonate-brine system has not been proven experimentally. Pure carbonate melt inclusions were also not found (the brine portion contains only rare carbonates). Compositions of all liquids are plotted on diagram of Fig. 9. The fluid phase is not distinct, because of the difficulties in its identification. However, the boundaries of the miscibility gap for fluid at $P > 25$ kbar can be outlined from Fig. 4. They are indicated in Fig. 9 by dashed lines, whereas the tie-lines connect the possible compositions of coexisting liquid phases, i.e., the silicate melt (kimberlite/lamproite proposed by Israeli et al., in press), the fluid, and the brine. In accordance with Fig. 4, it can be assumed that the miscibility gap disappears or appreciably narrows, displacing toward alkali-poor silicate melts. Such compositions correspond to the pyroxene–garnet rocks of the diamond-bearing Kumdy-Kol area of the Kokchetav Complex in northern Kazakhstan.

7. Conclusions

The reviewed experimental and natural data indicate the following phase relationships involving *KCpx* and melt:

(1) *KCpx* of at least 1 wt.% of K_2O may crystallize on the liquidus of relatively high-potassic silicate and carbonate–silicate melts at $P > 70$ kbar.

(2) K_p depends mostly on P and the SiO_2 content of the melt, but $K_p < 1$ for any bulk composition.

(3) The existing experimental data on dependence of K_p on pressure and the melt compositions were used to derive an equation for the P calculations from the compositions of *KCpx* and the coexisting silicate melt.

(4) The data on fluid inclusion from natural diamonds suggest that the deep-seated magma splits at $P < 50$ kbar into three liquids, i.e., silicate melt, a CO_2–H_2O–potassium-rich fluid, and a potassium-rich brine.

(5) The *KCpx* inclusions ($K_2O > 1.2$ wt.%) in garnet from ultra-high P potassium-poor rocks ($K_2O < 0.2$ wt.%) from the Kokchetav massif could have resulted from the crystallization of pyroxene on the liquidus of a silicate magma, which mixed or coexisted with potassium-rich brine at depth of about 250 km. Liquid immiscibility between the silicate melts and brine occurring during uplift resulted in a decrease of alkali activity in the silicate melt and a decrease of K_2O content in *Cpx*. The *Kfs* blebs observed in cores of coarse-grained clinopyroxenes may have resulted from the peritectic reaction $KCpx + melt = Di + Kfs$ at $P \sim 50-45$ kbar during the uplift.

Mineral and phase abbreviations used in the text

Abbreviation	Formula	Name of mineral
Ab	$NaAlSi_3O_8$	albite
Aeg	$NaFeSi_2O_6$	aegerine
Alm	$Fe_3Al_2Si_3O_{12}$	almandine
An	$CaAl_2Si_2O_8$	anorthite
APhl	$KMg_3AlSi_3O_{11}$	anhydrous phlogopite
Cal	$CaCO_3$	calcite
Cpx		clinopyroxene solid solution
Cos	SiO_2	coesite
Di	$CaMgSi_2O_6$	diopside
En	$Mg_2Si_2O_6$	enstatite
Esk	$Ca_{0.5}AlSi_2O_6$	Ca-Eskola pyroxene
Fs	$Fe_2Si_2O_6$	ferrosilite
Fo	Mg_2SiO_4	forsterite
Grs	$Ca_3Al_2Si_3O_{12}$	grossular
Grt		garnet solid solution
Hed	$CaFeSi_2O_6$	hedenbergite
Jd	$NaAlSi_2O_6$	jadeite
KCpx		potassium-bearing clinopyroxene
Kfs	$KAlSi_3O_8$	K-feldspar
KJd	$KAlSi_2O_6$	fictive K-jadeite
Ko	$NaCrSi_2O_6$	kosmochlor
Ks	$KAlSiO_4$	kalsilite

Ms	$KAl_3Si_3O_{10}(OH)_2$	muscovite
Nc	Na_2CO_3	Na-carbonate
Ne	$NaAlSiO_4$	nepheline
Ol		olivine solid solution
Opx		orthopyroxene solid solution
Phl	$KMg_3AlSi_3O_{10}(OH)_2$	phlogopite
Pl		plagioclase solid solution
Prp	$Mg_3Al_2Si_3O_{12}$	pyrope
Qtz	SiO_2	quartz
Rt	TiO_2	rutile
San	$KAlSi_3O_8$	sanidine
Tsc	$CaAl_2SiO_6$	Ca-Tschermak pyroxene
L_c		carbonate liquid
L_{Si}		silicate liquid
fl		fluid

Thermodynamic symbols used in the text

T	temperature
P	pressure
X_i^j	mole fraction of an *i*-component in a mineral *j*,
$N_i = 100X_i$	mol%
a_i	activity of an *i*-component
K_p	partition coefficient
K_r	reaction constant
ΔG_r^0	free energy difference in reaction r
ΔH_r^0	enthalpy difference in reaction r
ΔS_r^0	entropy difference in reaction r
ΔV_r^0	volume difference in reaction r
G_i^e	excess free energy of mixing of an *i*-component
R	gas constant (8.31 J/mol/K)

Acknowledgements

This work was financially supported by the Russian Foundation for Basic Research (projects 01-05-64775 and 01-05-06139 to OGS, and 99-05-65451 to VOY, 99-05-65602, 00-15-98519 "Leading Russian Scientific Schools" to LLP). We thank V.S. Shatsky for presenting the back-scattered image of *KCpx* mantled by glass (Fig. 10), and Oded Navon for sending us the unpublished analytical data on brines from diamonds. Review by Tibor Gasparik and an anonymous reviewer significantly improved the final version of this paper. Discussion of the thermodynamic model with Taras Gerya was very fruitful. Comments by Jan Kramers to an early version of this paper are greatly appreciated.

References

Bishop, F.C., Smith, J.V., Dawson, J.B., 1978. Na, K, P and Ti in garnet, pyroxene and olivine from peridotite and eclogite xenoliths from African kimberlites. Lithos 11, 155–173.

Borzdov, Yu.M., Sokol, A.G., Pal'yanov, Yu.N., Kalinin, A.A., Sobolev, N.V., 1999. Study of diamond crystallization in alkalic silicate, carbonate and carbonate–silicate melts. Dokl. Ross. Akad. Nauk, Earth Sci. 366, 530–533 (in Russian).

Chen, F., Guo, J.G., Chen, J.C., Liu, C.R., 1992. First discovery of high-potassium and high-chlorine in inclusions in diamond. Chin. Sci. Bull. 37, 1557–1560.

Dawson, J.B., 1989. Sodium carbonate lavas from Oldoinyo Lengai, Tanganyika: implications for carbonatite complex genesis. In: Bell, K. Carbonatites. Unwin Hyman, London, pp. 256–277.

Dawson, J.B., Garson, M.S., Roberts, B., 1987. Altered former carbonatite lava from Oldoinyo Lengal, Tanganyika: inferences for calcite carbonatite lavas. Geology 15, 765–768.

De Corte, K., Cartigny, P., Shatsky, V.S., Sobolev, N.V., Javoy, M., 1998. Evidence of fluid inclusions in metamorphic microdiamonds from the Kokchetav massif, northern Kazakhstan. Geochim. Cosmochim. Acta 62, 3765–3773.

Edgar, A.D., Mitchell, R.H., 1997. Ultra high pressure–temperature melting experiments on an SiO_2-rich lamproite from Smoky Butte, Montana: derivation of siliceous lamproite magmas from enriched sources deep in the continental mantle. J. Petrol. 38, 457–477.

Edgar, A.D., Vukadinovic, D., 1993. Potassium-rich clinopyroxene in the mantle: an experimental investigation of K-rich lamproite up to 60 kbar. Geochim. Cosmochim. Acta 57, 5063–5072.

Edgar, A.D., Charbonneau, H.E., Mitchell, R.H., 1992. Phase relations in an armalcolite–phlogopite lamproite from Smoky Butte, Montana: applications to lamproite genesis. J. Petrol. 33, 505–520.

Erlank, A.J., Kushiro, I., 1970. Potassium contents of synthetic pyroxenes at high temperatures and pressures. Carnegie Inst. Washington, Year Book 68, 267–271.

Freestone, I.C., Hamilton, D.L., 1980. The role of liquid immiscibility in the genesis of carbonatites. Contrib. Mineral. Petrol. 73, 105–117.

Gasparik, T., 1996. Melting experiments on the enstatite-diopside join at 70–224 kbar, including the melting of diopside. Contrib. Mineral. Petrol. 124, 139–153.

Harlow, G.E., 1996. Structure refinement of a natural K-rich diopside: the effect of K on the average structure. Am. Mineral. 81, 233–236.

Harlow, G.E., 1997. K in clinopyroxene at high pressure and temperature: an experimental study. Am. Mineral. 82, 259–269.

Harlow, G.E., Veblen, D.R., 1991. Potassium in clinopyroxene inclusions from diamonds. Science 251, 652–655.

Izraeli, E., Schrauder, M., Navon, O., 1998. On the connection between fluids and mineral inclusions in diamonds. Extended Abstracts, 7th International Kimberlite Conference, Cape Town, pp. 352–354.

Izraeli, E.S., Harris, J.W., Navon, O., 1999. Raman barometry of diamond formation. Earth Planet. Sci. Lett. 173, 351–360.

Izraeli, E.S., Harris, J.W., Navon, O., 2001. Brine inclusions in diamonds: a new upper mantle fluid. Earth Planet. Sci. Lett. 5807, 1–10.

Jones, A.P, Taniguchi, T., Dobson, D., Rabe, R., Milledge, H.J., Taylor, W.R., 1995. Experimental nucleation and growth of diamond from carbonate graphite system. 6th Int. Kimberlite Conference Extensional Abstracts, Novosibirsk, Russia, pp. 269–270.

Kogarko, L.N., Henderson, C.M.B., Kjarsgaard, B.A., 1991. Na-rich carbonate inclusion in perovskite and calzirite from the Guli intrusive Ca-carbonatite, Polar Siberia. Contrib. Mineral. Petrol. 109, 124–129.

Konzett, J., Ulmer, P., 1999. The stability of hydrous potassic phases in lherzolitic mantle—an experimental study to 9.5 GPa in simplified and natural bulk compositions. J. Petrol. 40, 629–652.

Koster van Groos, A.F., Wyllie, P.J., 1968. Melting relationships in the system $NaAlSi_3O_8$-NaF-H_2O to 4 kilobars pressure. J. Geol. 76, 50–70.

Koster van Groos, A.F., Wyllie, P.J., 1969. Melting relationships in the system NaAlSi$_3$O8-NaCl-H_2O at 1 kilobar pressure, with petrological applications. J. Geol. 77, 581–605.

Koster van Groos, A.F., Wyllie, P.J., 1973. Liquid immiscibility in the join $NaAlS_3O_8$-$CaAl_2Si_2O_8$-Na_2CO_3-H_2O. Am. J. Sci. 273, 465–487.

Kushiro, I., 1980. Changes with pressure and degree of partial melting and K_2O content of liquids in the system Mg_2SiO_4-KAlSiO4-SiO_2. Carnegie Inst. Washington, Year Book 79, 267–271.

Lavrova, L.D., Pechnikov, V.A., Pleshakov, A.M., Nadezhdina, Yu.A., Shukolyukov, Yu.A., 1999. A New Genetic Type of Diamond Deposit. Scientific World, Moscow.

Lee, W.-J., Wyllie, P.J., 1997. Liquid immiscibility between nephelinite and carbonatite from 1.0 to 2.5 GPa compared with mantle melt compositions. Contrib. Mineral. Petrol. 127, 1–16.

Lee, W.-J., Wyllie, P.J., 1998. Processes of crustal carbonatite formation by liquid immiscibility and differentiation, elucidated by model system. J. Petrol. 39, 2005–2013.

Litvin, Yu.A., Chudinovskih, L.T., Zharikov, V.A., 1997. Crystallization of diamond and graphite in mantle alkali carbonate melts in experiment at 7–11 GPa. Dokl. Ross. Akad. Nauk, Earth Sci. 355, 679–772.

Luth, R.W., 1992. Potassium in clinopyroxene at high pressure: experimental constraints. EOS, Trans. Am. Geophys. Union 73, 608.

Luth, R.W., 1995. Potassium in clinopyroxene at high pressure. EOS, Trans. Am. Geophys. Union 76, F711.

Luth, R.W., 1997. Experimental study of the system phlogopite-diopside from 3.5 to 17 GPa. Am. Mineral. 82, 1198–1209.

Matveev, Y.A., Litvin, Y.A., Perchuk, L.L., Chudinovskikh, L.T., Yapaskurt, V.O., 1998. Intensive carbonate–silicate reactions in the $K_2Mg(CO_3)_2$-$(Ca_{0.5}Mg_{0.5})SiO_3$-Al_2O_3 system in experiment at 7 GPa: relation to Kokchetav-type diamond deposits. Terra Nova 10 (Supplement No. 1), 39, Terra Abstracts.

McGregor, I.D., Carter, J.L., 1970. The chemistry of clinopyroxenes and garnets of eclogite and peridotite xenoliths from the Roberts Victor mine, South Africa. Phys. Earth Planet. Inter. 3, 391–397.

Mitchell, R.H., 1995. Melting experiments on a sanidine-phlogopite lamproite at 4–7 GPa and their bearing on the source of lamproitic magmas. J. Petrol. 36, 1455–1474.

Moore, J.D., Gurney, J.J., 1985. Pyroxene solid solution in garnets included in diamond. Nature 318, 582–584.

Navon, O., 1991. Infrared determination of high internal pressure in diamond fluid inclusions. Nature 353, 746–748.

Navon, O., 1999. Formation of diamonds in the Earth's Mantle. In: Gurney, J.J., Gurney, J.L., Pasque, M.D., Richardson, S.H. Proc. of the VIIth International Kimberlitic Conference, Red Roof Design, Cape Town, South Africa, pp. 584–604.

Navon, O., Izraeli, E.S., 1999. Cl- and K-rich micro-inclusions in cloudy diamonds. EOS, Trans. Am. Geophys. Union 80, F1128.

Navon, O., Hitcheon, I.D., Rossman, G.R., Wasserburg, G.J., 1988. Mantle-derived fluids in diamond microinclusions. Nature 325, 784–789.

Nielsen, T.F.D., Solovova, I.P., Veksler, I.V., 1997. Parental melts of melilitolite and origin of alkaline carbonatite: evidence from crystallized melt inclusions, Gardiner complex. Contrib. Mineral. Petrol. 126, 331–344.

Okamoto, K., Maruyama, S., 1998. Multi-anvil re-equilibration experiments of a Dabie Shan ultra-high pressure eclogite within the diamond-stability fields. Isl. Arc 7, 52–69.

Pal'yanov, Yu.N., Sokol, A.G., Borzdov, Yu.M., Khokhryakov, N.V., Sobolev, N.V., 1998. Diamond crystallization in the systems $CaCO_3$-C, $MgCO_3$C, $CaMg(CO_3)_2$C. Dokl. Ross. Akad. Nauk, Earth Sci. 363, 230–233 (in Russian).

Pal'yanov, Yu.N., Sokol, A.G., Borzdov, Yu.M., Khokhryakov, N.V., Sobolev, N.V., 1999. Diamond formation from mantle carbonate fluids. Nature 400, 417–418.

Perchuk, L.L., 1971. Carbonatites as possible products of carbonation of basalt magmas. Geochemistry, Petrology and Mineralogy of Alkalic Rocks. Nauka, Moscow, pp. 72–77 (in Russian).

Perchuk, L.L., 1987. Studies of volcanic series related to the origin of some marginal sea floors. In: Mysen, B.O. Magmatic Processes: Physicochemical Principles. Geochemical Society, Special Publication, USA, pp. 209–230.

Perchuk, L.L., Lindsley, D.H., 1980a. Carbonation effect on peridotite melt. Dokl. Akad. Nauk SSSR 250, 932–934 (in Russian).

Perchuk, L.L., Lindsley, D.H., 1980b. Experimental investigation of carbonation of basalt magmas: a plagioclase model. Dokl. Akad. Nauk SSSR 250, 1232–1236 (in Russian).

Perchuk, L.L., Lindsley, D.M., 1982. Fluid–magma interaction at high pressure–temperature conditions. In: Akimoto, S., Maghnani, M.N. High Pressure Research in Geophysics. Advances of Earth's and Planet Sciences (Special Issue) vol. 22, pp. 251–257.

Perchuk, L.L., Yapaskurt, V.O., 1998. Mantle-derived ultrapotassic liquids. Russ. Geol. Geophys. 39, 1746–1755.

Perchuk, L.L., Yapaskurt, V.O., Okay, A., 1995. Comparative petrology of diamond-bearing metamorphic complexes. Petrology 3, 238–276.

Perchuk, L.L., Sobolev, N.V., Yapaskurt, V.O., Shatsky, V.S., 1996. Relics of potassium-bearing pyroxenes from diamond-free pyroxene–garnet rocks of the Kokchetav massif, northern Kasakhstan. Dokl. Ross. Akad. Nauk, Earth Sci. 348, 790–795 (in Russian).

Prinz, M., Manson, D.V., Hlava, P.F., Keil, K., 1975. Inclusions in diamonds: garnet lherzolite and eclogite assemblages. Phys. Chem. Earth 9, 797–815.

Reid, A.M., Brown, R.W., Dawson, J.B., Whitfield, G.G., Siebert, J.C., 1976. Garnet and pyroxene compositions in some diamondiferous eclogites. Contrib. Mineral. Petrol. 58, 203–220.

Ricard, R.S., Harris, J.W., Gurney, J.J., Cardoso, P., 1989. Mineral inclusions in diamonds from the Koffiefontein Mine. In: Ross, J., et al. Kimberlites and Related Rocks: Their Mantle/Crust Setting, Diamonds, and Diamond Exploration. Geological Soc. Australia Spec. Pub. 14, vol. 2. Blackwell, Carlton, Victoria, pp. 1054–1062.

Schairer, J.F., Bowen, N.L., 1955. The system K_2O-Al_2O_3-SiO_2. Am. J. Sci. 253, 681–746.

Schrauder, M., Navon, O., 1993. Solid carbon dioxide in a natural diamond. Nature 365, 42–44.

Schrauder, M., Navon, O., 1994. Hydrous and carbonatitic mantle fluids in fibrous diamonds from Jwaneng, Botswana. Geochim. Cosmochim. Acta 58, 761–771.

Schrauder, M., Navon, O., Harris, J.W., 1993. Carbonate and water-bearing fluids trapped in an octahedral peridotitic diamond. EOS, Trans. Am. Geophys. Union 74, 636.

Schrauder, M., Koeberl, C., Navon, O., 1996. Trace element analyses of fluid diamonds from Jwaneng, Botswana. Geochim. Cosmochim. Acta 60, 4711–4724.

Shatsky, V.S., Jagoutz, E., Sobolev, N.V., Kozmenko, O.A., Parkhomenko, V.S., Troesch, M., 1999. Geochemistry and age of ultrahigh pressure metamorphic rocks from the Kokchetav massif (Northern Kazakhstan). Contrib. Mineral. Petrol. 137, 185–205.

Shimizu, N., 1971. Potassium content of synthetic clinopyroxenes at high pressures and temperatures. Earth Planet. Sci. Lett. 11, 374–380.

Shimizu, N., 1974. An experimental study of the partitioning of K, Rb, Cs, Sc and Ba between clinopyroxene and liquid at high pressures. Geochim. Cosmochim. Acta 38, 1789–1798.

Sobolev, N.V., Shatsky, V.S., 1990. Diamond inclusions in garnets from metamorphic rocks: a new environment for diamond formation. Nature 343, 742–746.

Sokol, A.G., Pal'yanov, Yu.N., Borzdov, Yu.M., Khokhryakov, N.V., Sobolev, N.V., 1998. Diamond crystallization in melt Na_2CO_3. Dokl. Ross. Akad. Nauk, Earth Sci. 361, 388–391 (in Russian).

Sokol, A.G., Tomilenko, A.A., Pal'yanov, Yu.N., Borzdov, Yu.M., Pal'yanova, G.A., Khokhryakov, A.F., 2000. Fluid regime of diamond crystalization in carbonate–carbon systems. Eur. J. Mineral. 12, 367–375.

Solovova, L.P., Girnis, A.V., Ryabchikov, I.D., 1996. Inclusions of carbonate and silicate melts in minerals of alkali basaltoids from the East Pamirs. Petrology 4, 319–341.

Stachel, T., Brey, G.P., Harris, J.W., 2000. Kankan diamonds (Guinea) I: from the lithosphere down to the transition zone. Contrib. Mineral. Petrol. 140, 1–15.

Tsuruta, K., Takahashi, E., 1998. Melting study of an alkali basalt JB-1 up to 12.5 GPa: behavior of potassium in the deep mantle. Phys. Earth Planet. Inter. 107, 119–130.

Wang, W., Takahashi, E., 1999. Subsolidus and melting experiments of a K-rich basaltic composition to 27 GPa: implication for behavior of potassium in the mantle. Am. Mineral. 84, 357–361.

Wyllie, P.J., Lee, W.-J., 1998. Model system controls on conditions for formation of magnesiocarbonatite and calciocarbonatite magmas from mantle. J. Petrol. 39, 1885–1893.

Zedgenizov, D.A., Logvinova, A.M., Shatsky, V.S., Sobolev, N.V., 1998. Inclusions in microdiamonds from some Yakutian pipes. Dokl. Ross. Akad. Nauk, Earth Sci. 359, 74–76 (in Russian).